UPPSALA
UNIVERSITET

Digital Comprehensive Summaries of Uppsala Dissertations from the Faculty of Science and Technology 295

Quantum Chemical Studies of Chemotherapeutic Drug Cisplatin

Activation and Binding to DNA

JOHAN RABER

ACTA
UNIVERSITATIS
UPSALIENSIS
UPPSALA
2007

ISSN 1651-6214
ISBN 978-91-554-6868-2
urn:nbn:se:uu:diva-7824

Dissertation presented at Uppsala University to be publicly examined in B42, BMC, Husargatan 3, Uppsala, Friday, May 11, 2007 at 13:15 for the degree of Doctor of Philosophy. The examination will be conducted in English.

Abstract
Raber, J. 2007. Quantum Chemical Studies of Chemotherapeutic Drug Cisplatin. Activation and Binding to DNA. Acta Universitatis Upsaliensis. *Digital Comprehensive Summaries of Uppsala Dissertations from the Faculty of Science and Technology* 295. 74 pp. Uppsala. ISBN 978-91-554-6868-2.

The serendipitous discovery of the potent cytotoxic properties of cisplatin brought about a revolution in the treatment of certain types of cancer, but almost fifty years later, there still remain unknown areas in the chemistry of cisplatin. There are questions regarding which form of the drug reaches its DNA target, or why certain DNA sequences are more preferred than others for reaction with cisplatin. The work presented here aims to address some of these problems, using quantum chemical calculations to complement and interpret available experimental data.

Cisplatin's activation reactions are explored by Density Functional Theory (DFT) on two model systems, one solely using a self-consistent reaction field (SCRF) for modeling bulk water, and one including an additional partial solvation shell of water molecules. It is concluded that adding explicit solvation provides a better picture than using SCRF solvation alone. The energy surface supports the view that the active form of cisplatin is the monoaquated form.

The activation reactions of the cisplatin-derived drug, JM118, are investigated using DFT and SCRF calculations using three solvation model systems. The results show a slower rate of hydrolysis for the first reaction, and a faster rate for the second, suggesting diaquated JM118 as the main DNA binding form of the drug.

Diaquated cisplatin's first and second reaction with guanine and adenine are studied using DFT and SCRF solvation. Cisplatin's propensity toward guanine in the first substitution is explained by larger stabilisation energy for the initially formed complex and by favoured kinetics. For the second substitution, higher stability in complexation with guanine over adenine is ascribed as the main factor favouring guanine over adenine substitution. This provides the first explanation for the predominance of 1,2-d(GpG) over 1,2-d(ApG) adducts, and the direction specificity of the 1,2-d(ApG) adducts.

Keywords: cisplatin, quantum chemistry, DNA, density functional theory, activation, JM118, substitution reaction, Platinum, guanine, adenine, cytostatic drug, aquation, anation, activation

Johan Raber, Department of Cell and Molecular Biology, Molecular biophysics, Box 596, Uppsala University, SE-75124 Uppsala, Sweden

ISSN 1651-6214
ISBN 978-91-554-6868-2
urn:nbn:se:uu:diva-7824 (http://urn.kb.se/resolve?urn=urn:nbn:se:uu:diva-7824)

"I am so smart, ESS-EM-AR-TEE" — H. Simpson

List of Papers

This thesis is based on the following papers, which are referred to in the text by their Roman numerals.

I Raber J., Zhu C., and Eriksson L. A., The Activation of Anti-Cancer Drug Cisplatin – is the Activated Complex Fully Aquated? *Mol. Phys.*, **102**, 2537 – 2544, (2003).

II Raber J., Zhu C., and Eriksson L. A., Theoretical Study of Cisplatin Binding to DNA: The Importance of Initial Complex Stabilization, *J. Phys. Chem. B*, **109**, 11006-11015, (2005).

III Zhu C., Raber J., and Eriksson L. A., Hydrolysis Process of the Second Generation Platinum-Based Anticancer Drug cis-Amminedichlorocyclohexylamineplatinum(II), *J. Phys. Chem. B*, **109**, 12195 – 12205, (2005).

IV Raber J., Llano J., and Eriksson L. A., Density Functional Theory in Drug Design - the Chemistry of Anti-tumor Drug cis-Platin and Photoactive Psoralen Compounds., In *Quantum Medicinal Chemistry*, chapter 4, 113 – 153, L. P. Carloni, F. Alber, Eds., Wiley-VCH: Weinheim (2003).

Additional publications:

i Llano J., Raber J., Eriksson L. A., Theoretical Study of Phototoxic Reactions of Psoralens, *J. Photochem. Photobiol. A*, **154**, 235 – 243, (2003).

ii Patriksson A., Adams C., Kjeldsen F., Raber J., van der Spoel D. and Zubarev R. A.: Prediction of N-Ca Bond Cleavage Frequencies in Electron Capture Dissociation of Trp-cage Dications by Force-field Molecular Dynamics Simulations *Int. J. Mass Spectrom.*, **248**, 124 – 135, (2006).

Contents

Abbreviations

AO	Atomic orbital
BO	Born - Oppenheimmer
CFT	Crystal Field Theory
CI	Configuration Interaction
CPMD	Car-Parinello Molecular Dynamics
DFT	Density Functional Theory
DNA	Deoxyribose Nucleic Acid
ECP	Effective Core Potential
FO	Frontier Orbital
GC	Gradient Corrected
GGA	Generalised Gradient Approximation. Synonymous to GC.
HF	Hartree - Fock
HH	Head-to-Head
HK	Hohenberg - Kohn
HT	Head-to-Tail
HMG	High Mobility Group
IEF-PCM	Integral Equation Formalism - PCM. See PCM below.
KS	Kohn - Sham
LDA	Local Density Approximation
LSDA	Local Spin Density Approximation
MD	Molecular Dynamics
MO	Molecular Orbital
MO-LCAO	MOs as Linear Combinations of Atomic Orbitals
NMR	Nuclear Magnetic Resonance
PC	Product Complex
PCM	Polarisable Continuum Model
PES	Potential Energy Surface
QM/MM	Quantum Mechanic / Molecular Mechanic

RC	Reactant Complex
RHF	Restricted Hartree - Fock
SAR	Structure - Activity Relationships
SCF	Self Consistent Field
S_N2	Bimolecular Nucleophilic Substitution
TS	Transition State

1. Introduction

Cisplatin and its derivative drugs have served as dependable cancer treatment agents over the past thirty years. The curing rate of cisplatin versus certain types of tumours[†] is a remarkable ~ 90% and thus cisplatin has become a very popular anti-cancer agent.[1] Nevertheless, there are drawbacks and shortcomings associated with its use; like all cytotoxins it is toxic after all. Side effects include nausea, risk of renal failure, and more importantly, native and aquired resistance to cisplatin by the tumour cells and consequentially the somewhat limited spectrum of tumour types which can be treated with cisplatin. Since these cisplatin associated problems have been well known since the start of cisplatin's clinical usage three decades ago, one may however find it surprising that subsequent generations of the drug are only marginally altered with respect to the parent compound. The largest change over the original compound introduced in second generation drug Carboplatin was the exchange of cisplatins chloride ligands for a dicarboxylate group[‡].

This seemingly snail like rate of development can partly be explained by the general success of cisplatin; a cancer drug with 90 % curing rate is impressive. In addition, there were two very influential papers[2,3] published on the Structure-Activity Relationships (SAR) of square planar metal complexes, which, at least superficially, appear to have narrowed the view of many researchers in the field. Among other things these SAR rules state that the square planar compound should be neutral (to pass through cell walls), have leaving ligands in a *cis*- arrangement around the coordinating metal center. The ligands should furthermore be of a type with susceptibility to substitution in a "window of reactivity" approximately centered around chloride and the coordinating metal should be Platinum(II). None of the subsequently released generations of the drug have broken these rules. A not too far fetched interpretation is that researchers have mainly looked within the boundaries set by the SAR rules.

Whether or not this is the case, no significantly more effective cisplatin derived compound has been developed and released to market as yet. This is where computational chemistry can be leveraged, as in this work,

[†]For instance testicular, ovarian and head and neck cancers. All of which are solid type tumours.

[‡]This is however not a *trivial* change since this simple substitution of two ligands drastically reduced the toxicity of cisplatin, thereby permitting higher dosage and lower, or no need for co-administration of protective medication.

to broaden the knowledge on cisplatins mode of action through basic research, expanding the body of knowledge for the benefit of the "hands on" developers of improved cisplatin derivatives.

Quantum chemistry, a sub-discipline of computational chemistry, is the weapon of choice when detailed knowledge of a chemical reaction is required and when it is impractical or even impossible to experimentally obtain the sought information. Quantum chemistry starts in 1927 with the valence bond theory of Heitler and London,[4] whose calculations on the hydrogen molecule are generally recognized as the first quantum chemical calculations. The field is greatly broadened and expanded in the fifties with the advent of computers and a therefore adapted theoretical framework, chiefly the Roothaan-Hall equations,[5,6] molding the groundwork laid by Hartree, Slater and Fock[7–9] in the late twenties in a form suitable for numerical computations. Of more recent date is the development during the sixties of modern Density Functional Theory (DFT), recasting the work done by Thomas, Fermi and Dirac[10–13] in the late twenties into a theory of passable accuracy for certain problems. The range of problems treatable by DFT was then vastly expanded in the late eighties and early nineties through the introduction of much improved functionals which enabled the treatment of *molecules* to chemical accuracy, and for that it today offers a very good[†] trade-off between computational expense and the preciseness of obtained results.

By necessity, quantum chemistry includes the electrons of the system in an explicit manner. Computationally, electrons are very cumbersome to treat due to their wave properties and their non-negligible mutual interactions. The size of the systems possible to study is consequently limited and therefore, when the chemical reaction of interest involves macromolecules, forces the use of size-reduced model systems to capture the essential chemistry of the larger system it models. This is the approach used in this work in the study of cisplatin's interactions with DNA, the quintessential macromolecule.

This thesis consists of two parts. The first part briefly describes the underlying theory permitting the quantified analysis offered by quantum chemistry. Basically how quantum mechanics applies to chemistry and computations. The second part details various aspects of the chemistry of cisplatin plus a small dose of its somewhat checkered history and in addition its clinical mode of action. Last in this second part the author's contributions in this field are summarized and a future outlook on cisplatin investigations is offered.

[†]For larger systems it is easy to argue it is the *best*.

2. Quantum chemistry

Ultimately, chemistry is a scientific discipline dealing with the motions and rearrangements of electrons in the electric field of atomic nuclei, motions which are governed by the laws of physics. Quantum chemistry is the branch of chemistry which provides a quantitative description of this electronic motion – the electronic structure, or wave function – founded on the postulates and physical principles of quantum mechanics. Knowing the electronic structure of a system in principle allows all chemical properties of the system to be determined. Not only that, it allows good or even excellent approximations to be made about the physical properties of the system through the molecular partition function, an approximation of which can be obtained once the electronic structure is known.

This chapter briefly presents the two major "schools of thought" in electronic structure theory – wave mechanics and density functional theory – and is by no means intended to be exhaustive in either scope or depth. That is the stuff of textbooks, for instance those referred to below. Note that for brevity, all equations herein are presented using atomic units unless otherwise explicitly stated.

The material in this chapter of the thesis has been compiled and adapted mainly from four textbooks [14–17] on the subject and references to original work have only been included for some of the major articles used in the present work. Complete references can however be found in almost any textbook on computational chemistry.

2.1 The Schrödinger equation

Within quantum chemistry there are different approaches to determine the electronic structure of an atom or molecule, but they all by different means solve the Schrödinger eigenvalue equation:

$$\hat{H}\Psi(\mathbf{r}) = E\Psi(\mathbf{r}). \tag{2.1.1}$$

In the wave mechanics formulation $\hat{H}$ is the Hamilton operator, $\Psi(\mathbf{r})$ is a wave function and E is a scalar representing the energy of the system. There are several formulations of this equation but the one referred to here and the following sections is the *time independent, non-relativistic* electronic Schrödinger equation. The Hamilton operator of a system with N electrons

and M nuclei is defined as

$$\hat{H} = -\frac{1}{2}\sum_{i=1}^{N}\nabla_i^2 - \sum_{i=1}^{N}\sum_{k=1}^{M}\frac{Z_k}{|\mathbf{r}_i - \mathbf{R}_k|} + \sum_{i=1}^{N}\sum_{j>i}^{N}\frac{1}{|\mathbf{r}_i - \mathbf{r}_j|}, \tag{2.1.2}$$

where ∇^2 is a differential operator ($\frac{\partial^2}{\partial x^2} + \frac{\partial^2}{\partial y^2} + \frac{\partial^2}{\partial z^2}$, in Cartesian coordinates), Z_k is the charge of nucleus k. The positions of the nuclei and electrons are indicated by $\mathbf{R}_k$ and $\mathbf{r}_{i,j}$ respectively. Schrödinger's equation takes the form of an eigenvalue equation where the Hamiltonian acting on the wave function produces a number, the energy of the system (E), times the retained wave function. The form of the Hamiltonian is an extension of the classical version for quantum mechanics, and is needed to account for the wave-particle duality of electrons. The first term on the right hand side of Eq. (2.1.2) is a sum of differential operators, ∇^2, which, when acting on the N electrons of the wave function $\Psi(\mathbf{r})$, produces the total kinetic energy of the system's electrons. The two double sums of the Hamiltonian describe the electrons interacting with the M nuclei and the electron-electron interactions respectively.

The solution to the Schrödinger equation thus involves finding the correct wave function of the system, which can be a daunting task indeed, since an infinite number of wave functions can be constructed which satisfies Eq. (2.1.1). Fortunately, there is a guiding light as to which wave function to choose, and it is called the variation principle. The variation principle states that, for a ground state wave function, any trial wave function will have an energy eigenvalue higher or equal to the exact energy of the ground state (corresponding to the exact wave function). In mathematical terms this means

$$E_{tr} = \frac{\int \Psi_{tr}^* \hat{H} \Psi_{tr} \mathrm{d}\mathbf{r}}{\int \Psi_{tr}^* \Psi_{tr} \mathrm{d}\mathbf{r}} = \frac{\langle \Psi_{tr} | \hat{H} | \Psi_{tr} \rangle}{\langle \Psi_{tr} | \Psi_{tr} \rangle} \geqslant E_{exact}. \tag{2.1.3}$$

Ψ_{tr} is the trial wave function and the asterisk denotes its complex conjugate. In the second equality the abstract *bra-ket* notation has been used where the *bra*, $\langle \cdots |$, denotes the complex conjugate transpose wave function[†] of the *ket*, $| \cdots \rangle$. The full bracket represents integration over all space. The denominator in the expressions is a normalisation factor. For normalised wave functions the denominator would equal one and the numerator accordingly would express the total energy of the wave function as the expectation value of the system Hamiltonian. The proof of the variation principle is given in Eq. (2.1.5) and should be read keeping the

[†]Strictly speaking the *bra* and the *ket* are states in general, each being the complex conjugate transpose of the other.

following properties of wave functions in mind:

$$\begin{aligned}
\left|\phi\right\rangle &= \sum_{\alpha} \left|\phi_\alpha\right\rangle \left\langle\phi_\alpha|\phi\right\rangle = \sum_{\alpha} \left|\phi_\alpha\right\rangle c_\alpha, \\
\left\langle\phi\right| &= \sum_{\alpha} \left\langle\phi|\phi_\alpha\right\rangle \left\langle\phi_\alpha\right| = \sum_{\alpha} c_\alpha^* \left\langle\phi_\alpha\right|, \\
\delta_{\alpha\beta} &= \left\langle\phi_\alpha|\phi_\beta\right\rangle.
\end{aligned} \tag{2.1.4}$$

This reads out as; if the state of a system $|\phi\rangle$ (and consequently its complex conjugate transpose $\langle\phi|$) is expanded in terms of eigenstates of the system, with expansion coefficients c_α and the eigenstates of the system being orthonormal, then the following must hold

$$\begin{aligned}
\left\langle\phi\right|\hat{H} - E_0\left|\phi\right\rangle &= \sum_{\alpha}\sum_{\beta} \left\langle\phi|\phi_\alpha\right\rangle \left\langle\phi_\alpha\right|\hat{H} - E_0\left|\phi_\beta\right\rangle \left\langle\phi_\beta|\phi\right\rangle \\
&= \sum_{\alpha}\sum_{\beta} c_\alpha^* c_\beta \left(E_\beta - E_0\right) \left\langle\phi_\alpha|\phi_\beta\right\rangle \\
&= \sum_{\alpha} |c_\alpha|^2 \left(E_\alpha - E_0\right) \geqslant 0,
\end{aligned} \tag{2.1.5}$$

where in the last expression both $|c_\alpha|^2$ and $(E_\alpha - E_0)$ are non-negative numbers for all indices α since $E_0 \leqslant E_1 \leqslant E_2 \leqslant \ldots \leqslant E_\infty$. The proof is almost trivial but it tells us something vitally important: We can *not* construct a wave function of lower energy than the correct ground state wave function of the system. This principle forms the basis of the method presented in section 2.3, variational minimisation of a trial estimate wave function to obtain an approximation to the true solution.

For poly-electronic systems, by far the most common form of the wave function used is that of the Slater determinant:

$$\Psi(\mathbf{r}) = \frac{1}{\sqrt{N!}} \begin{vmatrix} \phi_1(\mathbf{r}_1) & \phi_2(\mathbf{r}_1) & \cdots & \phi_N(\mathbf{r}_1) \\ \phi_1(\mathbf{r}_2) & \phi_2(\mathbf{r}_2) & \cdots & \phi_N(\mathbf{r}_2) \\ \vdots & \vdots & \ddots & \vdots \\ \phi_1(\mathbf{r}_N) & \phi_2(\mathbf{r}_N) & \cdots & \phi_N(\mathbf{r}_N) \end{vmatrix}. \tag{2.1.6}$$

In this expression, $\phi_n(\mathbf{r}_m)$ is wave function n of electron m having coordinates $\mathbf{r}_m$ and the factor preceding the matrix is a normalising factor which accounts for the indistinguishable nature of the electrons. This mathematical form fulfills the anti-symmetry requirement of fermionic system wave functions, which means that interchanging any two wave functions in the matrix changes the sign of $\Psi(\mathbf{r})$, and as a consequence it obeys the *Pauli exclusion principle*, meaning that if two electrons in the matrix have the same set of quantum numbers, and hence their wave functions are identical, the determinant is zero and the wave function vanishes.

Furthermore, since the Hamilton operator is Hermitian, we are free to chose the constituent wave functions orthonormal, $\langle\phi_i|\phi_j\rangle = \delta_{ij}$, which is

a mathematical necessity in the development of the Hartree-Fock method detailed in section 2.3. The constituent wave functions of the Slater determinant consist of a spatial part multiplied by a spin function (α or β, "spin up" or "spin down" respectively), e.g. $\phi_n(\mathbf{r}_m) = \psi_n(\mathbf{r}_m)\,\alpha$, and are referred to as spin orbitals.

When evaluating an expression of the (2.1.3) type, or rather $\langle\Psi|\hat{O}|\Psi\rangle$ in which $\hat{O}$ is any operator, $\langle\Psi|\hat{O}|\Psi\rangle$ is said to be the matrix representation of operator $\hat{O}$, that is

$$\hat{O} \doteq \langle\Psi|\hat{O}|\Psi\rangle = \begin{vmatrix} \langle\phi_1|\hat{O}|\phi_1\rangle & \langle\phi_1|\hat{O}|\phi_2\rangle & \cdots & \langle\phi_1|\hat{O}|\phi_N\rangle \\ \langle\phi_2|\hat{O}|\phi_1\rangle & \langle\phi_2|\hat{O}|\phi_2\rangle & \cdots & \langle\phi_2|\hat{O}|\phi_N\rangle \\ \vdots & \vdots & \ddots & \vdots \\ \langle\phi_N|\hat{O}|\phi_1\rangle & \langle\phi_N|\hat{O}|\phi_2\rangle & \cdots & \langle\phi_N|\hat{O}|\phi_N\rangle. \end{vmatrix} \tag{2.1.7}$$

When $\hat{O}$ is the Hamilton operator and Ψ is a Slater determinant, many of the matrix elements, $\langle\phi_i|\hat{H}|\phi_j\rangle$, of this matrix representation equal zero, thereby simplifying the search for the wave function and energy when solving the Schrödinger equation, which is the subject of section 2.3.

2.2 The Born-Oppenheimer approximation

For atoms, the Schrödinger equation can only be solved analytically for systems with one electron. Obviously, the solution to the Schrödinger equation becomes increasingly complex as more electrons are present. Consequently approximations must be made. The most important approximation is the Born-Oppenheimer approximation[18] which states that, under non-exotic conditions, a separation of the nuclear and electronic wave functions is valid:

$$\Psi_{tot}(\mathbf{R},\mathbf{r}) = \Psi_n(\mathbf{R},\mathbf{r})\,\Psi_e(\mathbf{R},\mathbf{r}). \tag{2.2.1}$$

In this expression, the total wave function $\Psi_{tot}(\mathbf{R},\mathbf{r})$ is simply the product of the nuclear and electronic wave function, $\Psi_n(\mathbf{R},\mathbf{r})$ and $\Psi_e(\mathbf{R},\mathbf{r})$ respectively, with $\mathbf{R}$ and $\mathbf{r}$ being the nuclear and electron coordinates. This says that, the nuclear wave function does not depend directly on the electronic wave function and vice-versa.

The full derivation leading to this approximation quantifies the extent to which the wave functions are coupled, in terms of their energy contribution to the total wave function, and defines a correction term for the error introduced by separating the electronic and nuclear wave functions. The magnitude of the correction term to the electronic contribution is in the order of the electron-nuclei mass ratio, which is always less than $\sim \frac{1}{1836}$. In effect, this means that because the inertial mass of the electrons is so much less than that of the nuclei, their movement is fast enough relative to the nuclei

that they are in a constant state of equilibrium with respect to them. The nuclei can consequently be considered fixed when solving the electronic Schrödinger equation.

In cases where the Born-Oppenheimer (BO) approximation is valid, the electronic Schrödinger equation can be solved independently of the nuclear Schrödinger equation

$$\hat{H}\Psi_e(\mathbf{r};\mathbf{R}) = E_e\Psi_e(\mathbf{r};\mathbf{R}). \tag{2.2.2}$$

Here, $\mathbf{R}$ only enters as a parameter and not a variable. Accordingly, the interaction energy between nuclei can be treated separately and nucleic motions are confined to a "Potential Energy Surface" (PES) created by the field of the electrons. Nucleus-nucleus interactions are now described as classical Coulomb interactions and not as wave functions.

The BO approximation is generally valid except under special conditions. For instance, the approximation can break down when the magnetic moments of the nuclei couple with that of the electrons in rapidly rotating diatomic molecules.

When the BO approximation is assumed valid, the Schrödinger equation of another one-electron system can be solved analytically: H_2^+ (or analogous one-electron diatomic systems). For poly-electronic systems though, there are no analytical solutions and iterative methods must be employed where the Schrödinger equation is solved one electron at a time. This is the subject of the following section.

2.3 The Self Consistent Field method

Even under the BO approximation the problem to find the electronic wave function solving the Schrödinger equation remains. The electrons have identical inertial masses and hence the wave functions of the individual electrons can not be immediately separated à la the BO approximation, since the magnitude of mutual electron-electron interaction is too large to permit such a separation. A cruder, yet subtle, approach is called for: The Self Consistent Field (SCF) method.

Upon inspection of the expression for the total energy of an electronic system, Eq. (2.1.2) and Eq. (2.1.3), it is evident that the resulting energy is composed of a one-electron contribution and a two-electron contribution. The Hamiltonian can thus be separated in a one-electron and a two-electron part. The one-electron Hamiltonian, denoted $\hat{H}^{core}$, has the form

$$\hat{H}^{core} = -\frac{1}{2}\sum_{i=1}^{N}\nabla_i^2 - \sum_{i=1}^{N}\sum_{k=1}^{M}\frac{Z_k}{|\mathbf{r}_i - \mathbf{R}_k|}, \tag{2.3.1}$$

in which index i refer to the electrons and k to the nuclei. The denominator of the double sum, $|\mathbf{r}_i - \mathbf{R}_k|$, is the distance between the electrons and the

nuclei and Z_k is the charge of nucleus k. $\hat{H}^{core}$ would give a complete description of the system assuming non-interacting electrons. Naturally, electrons do interact, and the nature of this interaction must be determined in order to proceed with the solution of the Schrödinger equation.

The two-electron part of the Hamiltonian then accordingly becomes

$$\hat{H}^{ee} = \sum_{i}^{N} \sum_{j>i}^{N} \frac{1}{\left|\mathbf{r}_i - \mathbf{r}_j\right|} = \sum_{i,j} \mathbf{r}_{ij}^{-1}, \quad \text{with} \quad \mathbf{r}_{ij} = \left|\mathbf{r}_i - \mathbf{r}_j\right|, \tag{2.3.2}$$

in which indices i and j refer to different electrons and the double sum consequently runs over all *pairs* of electrons.

Since the Hamilton operator is Hermitian, we can choose the spin orbitals of the Slater determinant to be orthonormal. This brings a host of mathematical conveniences to our solving the Schrödinger equation. For one it lets us evaluate the energy expectation value of $\hat{H}^{core}$ as $\langle \hat{H}^{core} \rangle = \sum_i^N \langle \phi_i(\mathbf{r}_1) | \hat{H}^{core} | \phi_i(\mathbf{r}_1) \rangle$. Furthermore, the expansion of Eq. (2.1.3) with respect to electron-electron interactions in the Hamiltonian, $\langle \Psi | \hat{H}^{ee} | \Psi \rangle = \langle \Psi | \mathbf{r}_{ij}^{-1} | \Psi \rangle$, leads to most of the matrix element terms of the expansion being zero, due to this orthogonality. The two-electron matrix elements have the general appearance

$$\langle \phi_i(\mathbf{r}_1)\phi_j(\mathbf{r}_2) | \hat{O}_2 | \phi_k(\mathbf{r}_1)\phi_l(\mathbf{r}_2) \rangle = \langle ij | kl \rangle, \tag{2.3.3}$$

where the right hand side is a conventional short hand notation of the left hand side in which $\hat{O}_2$ is a general two-electron operator acting on any pair of electrons 1 and 2 in spin-orbitals i, j, k and l. For Coulomb interactions between electrons; $\hat{O}_2 = \hat{H}^{ee} = |\mathbf{r}_1 - \mathbf{r}_2|^{-1} = \mathbf{r}_{12}^{-1}$. The non-zero matrix elements of $\hat{H}^{ee}$ are of two types. The first one is denoted:

$$\begin{aligned} J_{ij} &= \langle ij | \mathbf{r}_{12}^{-1} | ij \rangle = \iint \phi_i^*(\mathbf{r}_1)\phi_j^*(\mathbf{r}_2) \frac{1}{\mathbf{r}_{12}} \phi_i(\mathbf{r}_1)\phi_j(\mathbf{r}_2) \mathrm{d}\mathbf{r}_1 \mathrm{d}\mathbf{r}_2 \\ &= \iint \left|\phi_i(\mathbf{r}_1)\right|^2 \frac{1}{\mathbf{r}_{12}} \left|\phi_j(\mathbf{r}_2)\right|^2 \mathrm{d}\mathbf{r}_1 \mathrm{d}\mathbf{r}_2. \end{aligned} \tag{2.3.4}$$

This term is called a Coulomb element and represents the repulsion between two electrons in different molecular orbitals, analogous to the classical expression. It is in fact identical to it when using the interpretation of $\left|\phi_i(\mathbf{r}_1)\right|^2$ as a charge density. The total Coulomb contribution of an electron in orbital ϕ_i to the total electronic energy then becomes

$$E_i^C = \sum_{j \neq i}^{N} \langle ij | \mathbf{r}_{12}^{-1} | ij \rangle = \sum_{j \neq i}^{N} J_{ij}. \tag{2.3.5}$$

The total Coulombic contribution from all electrons of the system then becomes a double sum

$$E_{tot}^C = \sum_{i=1}^{N} \sum_{j=i+1}^{N} \langle ij | \mathbf{r}_{12}^{-1} | ij \rangle = \sum_{i=1}^{N} \sum_{j=i+1}^{N} J_{ij}. \tag{2.3.6}$$

The second type of term that survives the expansion of the Slater determinant is a different beast altogether, and it entails the first non-classical effect this far. It is important to note that the Slater determinant is constructed such, that every electron of the determinant is present in every spin orbital ϕ_i, which has the consequence that another non-vanishing term for electron-electron interactions appears in the expansion. The term represents a correction to the Coulomb interactions for the fact that quantum particles are indistinguishable and that every electron can occupy any spin orbital. This term is called the exchange term and has the form

$$K_{ij} = \left\langle ij \middle| \mathbf{r}_{12}^{-1} \middle| ji \right\rangle = \iint \phi_i^*(\mathbf{r}_1)\phi_j^*(\mathbf{r}_2)\frac{1}{\mathbf{r}_{12}}\phi_j(\mathbf{r}_1)\phi_i(\mathbf{r}_2)\mathrm{d}\mathbf{r}_1\mathrm{d}\mathbf{r}_2. \tag{2.3.7}$$

Note that the electrons one and two are present in both ϕ_i and ϕ_j in the integral, that is they are exchanged, hence the name of the term. Also observe that K_{ij} only exists for electrons of the same spin, and consequently ϕ_i and ϕ_j in Eq. (2.3.7) are the spatial parts of spin orbitals with equal spin. This is readily apparent comparing the expressions

$$\begin{aligned} K_{ij} &= \left\langle \phi_i(\mathbf{r}_1)\phi_j(\mathbf{r}_2) \middle| \mathbf{r}_{12}^{-1} \middle| \phi_j(\mathbf{r}_1)\phi_i(\mathbf{r}_2) \right\rangle \\ &= \iint \psi_i^*(\mathbf{r}_1)\alpha^*\psi_j^*(\mathbf{r}_2)\alpha^*\frac{1}{\mathbf{r}_{12}}\psi_j(\mathbf{r}_1)\alpha\psi_i(\mathbf{r}_2)\alpha\mathrm{d}\mathbf{r}_1\mathrm{d}\mathbf{r}_2 \\ &= \iint \psi_i^*(\mathbf{r}_1)\psi_i(\mathbf{r}_2)\left|\alpha\right|^2\frac{1}{\mathbf{r}_{12}}\psi_j^*(\mathbf{r}_2)\psi_j(\mathbf{r}_1)\left|\alpha\right|^2\mathrm{d}\mathbf{r}_1\mathrm{d}\mathbf{r}_2 \\ &= \iint \psi_i^*(\mathbf{r}_1)\psi_i(\mathbf{r}_2)\frac{1}{\mathbf{r}_{12}}\psi_j^*(\mathbf{r}_2)\psi_j(\mathbf{r}_1)\mathrm{d}\mathbf{r}_1\mathrm{d}\mathbf{r}_2 \end{aligned} \tag{2.3.8}$$

and

$$\begin{aligned} 0 &= \left\langle \phi_i(\mathbf{r}_1)\phi_j(\mathbf{r}_2) \middle| \mathbf{r}_{12}^{-1} \middle| \phi_j(\mathbf{r}_1)\phi_i(\mathbf{r}_2) \right\rangle \\ &= \iint \psi_i^*(\mathbf{r}_1)\alpha^*\psi_j^*(\mathbf{r}_2)\beta^*\frac{1}{\mathbf{r}_{12}}\psi_j(\mathbf{r}_1)\alpha\psi_i(\mathbf{r}_2)\beta\mathrm{d}\mathbf{r}_1\mathrm{d}\mathbf{r}_2 \\ &= \iint \psi_i^*(\mathbf{r}_1)\psi_i(\mathbf{r}_2)\alpha^*\beta\frac{1}{\mathbf{r}_{12}}\psi_j^*(\mathbf{r}_2)\psi_j(\mathbf{r}_1)\beta^*\alpha\mathrm{d}\mathbf{r}_1\mathrm{d}\mathbf{r}_2, \end{aligned} \tag{2.3.9}$$

where the third expression of Eq. (2.3.9) equals zero due to the orthogonality of α and β spin.

Owing to the antisymmetric nature of the Slater determinant, the exchange interaction gives a negative contribution to the total energy. It has no classical analogue and should be seen as a correction to the Coulomb repulsion term accounting for the Pauli principle, which dictates that two electrons of the wave function cannot have the same set of quantum numbers. Put differently, the exchange integral reduces the probability of finding two electrons with equal spin at the same point in space, since they in such case could be considered to have the same set of quantum numbers.

Having accounted for all interactions in the system, the total energy of the system can now be expressed as

$$E_{tot} = \sum_{i=1}^{N} H_i^{core} + \frac{1}{2}\sum_{i=1}^{N}\sum_{j=1}^{N}\left(J_{ij} - K_{ij}\right) + V_{nn}, \tag{2.3.10}$$

where V_{nn} is the classical expression for the repulsion of the nuclei. The factor $\frac{1}{2}$ accounts for the fact that the double sum, in this formulation, counts all electron pair interactions twice. Usually this expression for the total energy is rewritten in operator form to facilitate variational analysis

$$\begin{aligned} E_{tot} = &\sum_{i=1}^{N} \langle \phi_i | \hat{H}_i^{core} | \phi_i \rangle + \frac{1}{2}\sum_{i=1}^{N}\sum_{j=1}^{N}\left(\langle \phi_j | \hat{J}_i | \phi_j \rangle - \langle \phi_j | \hat{K}_i | \phi_j \rangle\right) \\ &+ \sum_{k=1}^{M}\sum_{l=1}^{M} \frac{Z_k Z_l}{|\mathbf{R}_k - \mathbf{R}_l|} \\ \hat{J}_i \left|\phi_j(\mathbf{r}_2)\right\rangle &= \left\langle \phi_i(\mathbf{r}_1) \middle| \mathbf{r}_{12}^{-1} \middle| \phi_i(\mathbf{r}_1) \right\rangle \left|\phi_j(\mathbf{r}_2)\right\rangle \\ \hat{K}_i \left|\phi_j(\mathbf{r}_2)\right\rangle &= \left\langle \phi_i(\mathbf{r}_1) \middle| \mathbf{r}_{12}^{-1} \middle| \phi_j(\mathbf{r}_1) \right\rangle \left|\phi_i(\mathbf{r}_2)\right\rangle. \end{aligned} \tag{2.3.11}$$

For a polyatomic system the most common approach for the variational analysis is to determine a linear combination of atomic orbitals (called Molecular Orbitals, MOs or sometimes MO-LCAO) that minimise the total electronic energy under the constraint that the MOs remain orthonormal. This can be accomplished by means of Lagrange multipliers. The derivations are omitted, but the result is that a *one-electron* operator, the Fock operator, acting on the *variation* of the energy, δE, can be determined. The interested reader can find an excellent derivation of the Hartree-Fock equations in the text book "*Modern Quantum Chemistry*" by Szabo and Ostlund.[14]

Defining the operator to work on δE as opposed to E directly is motivated by the variational principle, that is since we are looking for a stationary point, specifically a minimum of the wave function; δE should equal zero. This approach does not *guarantee* the stationary point found to be a minimum but normally this is the case, and the nature of the stationary point can always be checked when needed through the second order term $\delta^2 E$. The Fock operator is defined as:

$$\hat{F}_i = \hat{h}_i + \sum_{j}^{N}\left(\hat{J}_j - \hat{K}_j\right), \tag{2.3.12}$$

and is a one-electron operator working on orbital i in the mean, static field of the remaining electrons of orbitals $j \neq i$. Using this operator, the Hartree-Fock (HF) equations[7–9] can be obtained

$$\hat{F}_i \phi_i = \sum_{j}^{N} \lambda_{ij} \phi_j, \tag{2.3.13}$$

where λ_{ij} are Lagrange multipliers. A unitary transformation of the matrix of Lagrange multipliers can then be employed to transform the Hartree-Fock equations into a set of one-electron, pseudo-eigenvalue equations, the *canonical* HF equations;

$$\hat{F}_i \phi'_i = \varepsilon_i \phi'_i, \tag{2.3.14}$$

in which ϕ'_i is the transformed orbital ϕ_i and ε_i is the associated energy eigenvalue. The Fock operator depends on all other orbitals of the system and the HF equations must therefore be solved iteratively, since these are not known *a priori*. In practice, this means that a starting guess, or estimate, must be made and the orbitals (ϕ'_i) are updated under the assumption that the remaining orbitals are static. When the change in the wave function (or electron density) between two iterations fall below some desired level, the field made up of the orbitals is said to be self consistent, hence the name "Self Consistent Field" methods.

As mentioned above, the description of the wave functions in the Hartree-Fock equations are most often a linear combination of atomic orbitals (MO-LCAO), in which the molecular orbitals consists of basis functions like

$$\phi_i = \sum_{\alpha}^{Q} c_{\alpha i} \chi_\alpha, \tag{2.3.15}$$

where Q is the number of basis functions, for instance atomic orbitals. A common choice for χ, the basis functions, is a representation of the atomic orbitals as a linear combination of gaussian function primitives. This is elaborated on in section 2.3.1. In the wave function description of Eq. (2.3.15) the canonical HF equations become

$$\hat{F}_i \sum_{\alpha}^{Q} c_{\alpha i} \chi_\alpha = \varepsilon_i \sum_{\alpha}^{Q} c_{\alpha i} \chi_\alpha. \tag{2.3.16}$$

This far the HF equations are completely general and applies to any molecular wave function. In the common, specific case of a closed shell ground state wave function, the Fock equations in an atomic orbital basis (the Roothaan-Hall equations[5,6]) are obtained by multiplication from the left by the desired basis function and subsequently integrating over the basis functions. Integrating out spin from the spin-orbitals, leaving the spatial part of the orbitals, the Fock operator is redefined as:

$$f(1) = \hat{H}^{core}(1) + \sum_{j}^{Q/2} 2\hat{J}_j(1) - \hat{K}_j(1). \tag{2.3.17}$$

In matrix form the Roothaan-Hall equations become

$$\begin{aligned} &\mathbf{FC} = \mathbf{SC}\boldsymbol{\varepsilon} \\ &F_{\alpha\beta} = \langle \chi_\alpha | f(1) | \chi_\beta \rangle \\ &S_{\alpha\beta} = \langle \chi_\alpha | \chi_\beta \rangle. \end{aligned} \tag{2.3.18}$$

The matrix representation, **F**, of the Fock operator contains the Fock matrix elements $F_{\alpha\beta}$ and **S** is the matrix of all the overlap elements between basis functions χ_α and χ_β, that is $S_{\alpha\beta} = \int \chi_\alpha^* (\mathbf{r}_1)\, \chi_\beta (\mathbf{r}_1)\, \mathrm{d}\mathbf{r}_1$. Matrix **C** contains the coefficients of the linear combination of atomic orbitals. One thus seeks to find the matrix **C** which minimises the diagonal matrix $\boldsymbol{\varepsilon}$ containing the orbital energies. In line with the above discussion about the HF equations, the coefficients of matrix **C** have to be guessed or estimated initially, followed by iterative optimisation until self consistency is achieved.

2.3.1 Basis sets

The underlying assumption in the MO-LCAO formalism above is that a molecular wave function can be described as a superposition of individual wave functions of the constituent atoms of the molecule. Assuming that the entire Hilbert space of solutions to the atomic Schrödinger equation is known for the atoms of the molecule, MO-LCAO would also be an exact solution to the molecular problem. Unfortunately the atomic wave function Hilbert space is not known in general. Luckily though, this does not render the MO-LCAO approach useless since a sufficiently large portion of the atomic Hilbert space can be mapped to desired accuracy, thereby lending credence to the MO-LCAO proposition. The mapping is done by means of *basis functions*, referred to in the preceding section as χ, and a *basis set* comprises a collection of basis functions.

Originally basis functions were chosen resembling the solutions to the hydrogenic problem

$$\phi_i(\zeta, n, l, m; r, \theta, \varphi) = N r^{n-1} e^{-\zeta r} Y_l^m(\theta, \varphi), \tag{2.3.19}$$

which were called Slater Type Orbitals (STOs). In the STO; N is a normalisation factor, n is the principal quantum number, ζ is called "exponent" and Y_l^m are the spherical harmonics for angular quantum numbers l and m. The r, θ and φ are spherical coordinates. Theoretically the STO is a very attractive choice of basis function to represent the true AOs due to their similarity to the analytical solutions to the Schrödinger equation of the hydrogen atom. Slater type orbitals have long since fallen out of favour though, as the calculations are performed by computers and the STOs are unwieldy compared to the subsequently introduced Gaussian Type Orbital (GTO)

$$g\left(\alpha, l, m, n; x, y, z\right) = N e^{-\alpha r^2} x^l y^m z^n. \tag{2.3.20}$$

Here, N is a normalisation constant and α is called the "exponent". The l, m and n are *not* quantum numbers but they must obey the condition $L = l + m + n, \quad L = 0, 1, 2, \ldots$, where L is analogous to the angular momentum quantum number l of the STOs. The x, y and z are Cartesian coordinates and $r^2 = x^2 + y^2 + z^2$. It must be noted that GTOs are *not* proper orbitals

and are usually referred to as gaussian primitives. Originally they were used to represent STOs as a linear combination of a number of gaussian primitives. This practice was later abandoned in favour of fitting to highly accurate quantum Monte-Carlo calculated wave functions on larger systems (than the hydrogen atom).

Numerical evaluation of matrix elements and overlap integrals using GTOs is more than an order of magnitude faster than using STOs, which thus lets one STO be represented by a linear combination of more than ten GTOs at roughly equal computational cost. Since an STO can be adequately represented by well below ten GTOs[†], the GTOs are the preferred way to describe the wave function. This computational advantage becomes even more pronounced when using *contractions* of gaussian primitives to represent the true orbitals. A contraction basically is a linear combination of gaussian primitives with fixed exponents and coefficients. Obviously this reduces the flexibility of the wave function ultimately produced by variational minimisation and hence also the accuracy of the obtained wave function. Careful choice of contraction scheme can nevertheless reduce this drawback to acceptable levels.

There are two main ways in which contractions are formulated; segmented and general, of which the segmented type is by far the most commonly used. There is nothing inherently superior about the segmented type of basis set and its popularity is largely due to the historical lack of efficient implementation of the general contractions in the most popular quantum chemical software packages. In segmented contractions there is only one instance of each individual gaussian primitive used to represent the AO [‡], that is the contractions are disjoint, whereas in general contractions each primitive gaussian is present in all contractions. For either contraction scheme though, it holds that as more GTOs are used in a contraction, a higher accuracy is achieved. An infinitely large basis set is in this sense *complete*, becoming indistinguishably close to the "true" function. By the same token, any realistically usable basis set is therefore *incomplete*. When a basis set approach completeness, a limit is eventually reached – the basis set limit – where adding more gaussian primitives yields no improved accuracy. This limit is then imposed by the method used to obtain the wave function and in the Hartree-Fock case this is called – quite naturally – the "Hartree-Fock limit".

There is an unfortunate side effect to the basis set limit, apart from the reduction in absolute accuracy of the wave function, called the basis set superposition error (BSSE). It arises as a consequence of basis set incompleteness and is especially evident when studying weak interactions

[†]Six GTOs is a common figure for the most difficult case, the 1s orbital, with its lack of cusp at $r = 0$.

[‡]There are exceptions where one or two gaussian primitives appear in more than one contraction, but this is not the common case.

such as van der Waals forces or hydrogen bonds in complexation reactions. In complexation, it appears since the basis functions of neighbouring molecule(s) in the complex are accessible to the wave function of all the complex constituents, thereby inevitably reducing the electronic energy of these molecules. This leads to an overestimation of the complexation energy.

A first step to reduce this error is to increase the size of the basis set used, provided the extra computational expense can be afforded, since BSSE is an effect of basis set incompleteness. Furthermore, the error can be approximated using the counterpoise correction (CP)

$$\Delta E_{CP} = E'_{ab}(A) + E'_{ab}(B) - E'_{a}(A) - E'_{b}(B), \tag{2.3.21}$$

here shown for a bimolecular complex. The first two terms of the right hand side sums the energies of individual molecules A and B in their bimolecular complex geometry, indicated by the prime, using the basis set functions ab of the entire complex AB. Subtracted from this sum are the energies of molecules A and B, in their bimolecular complex geometry, using only their "natively" accessible basis functions a and b. The counterpoise correction is subsequently added to the complexation energy.

A specific type of basis set that has been used extensively in this work is the Effective Core Potential (ECP) basis set. The ECP basis sets only include valence electrons explicitly and replaces the influence of the core electrons by a static, effective potential, commonly described by a polynomial function. The effective potential accounts for relativistic effects, which is the rationale for the introduction of the effective potential, and this tremendously reduces the computational expense for heavier elements where relativistic effects are significant for the core electrons of the atom.

2.4 Electron correlation in quantum chemistry

The restricted Hartree-Fock (RHF) formalism described above suffers from two inherent flaws. Both flaws are related to the correlation between electrons but are of different character, one is a short range effect and the other is a long range effect; they are called dynamic and non-dynamic (sometimes called static) correlation respectively. The definition of the correlation energy[19] is

$$E_{corr} = E_{exact} - E_{HF}. \tag{2.4.1}$$

As can be seen from Eq. (2.4.1), the correlation energy is defined as the difference between the exact energy and the HF energy even though the HF energy explicitly includes exchange energy, which is a correlation effect.

Dynamic correlation, or the more descriptive term Coulomb correlation, is a spatial correlation of the electrons' motion arising due to Coulomb repulsion. An example is that the two 1s electrons of the Helium atom, even

though their electronic density distributions are identical, are more likely to be found at opposite sides of the nucleus at any given time due to mutual repulsion. Single determinant wave function methods such as HF are ill equipped to address this and multi determinant methods or Density Functional Theory (see Section 2.5) must then be employed.

The error in RHF theory concerning non-dynamic correlation is the approximation that the wave function solving the Schrödinger equation is described by one Slater determinant *only*. The inaccuracy of this description is best illustrated by an example: Consider a molecule with two degenerate frontier orbitals (FO), that is a system where equivalent resonance structures can be found, and there are two electrons to put in the two FOs. Hund's rule (No. 2) states that the lowest energy of the wave function will be reached when the two electrons are placed one in each degenerate FO with parallel spin. This is not possible in the RHF formalism, and the two electrons will get paired spin and be put in one of the FOs. It is easily realised that an equally valid wave function could be constructed with the electrons occupying the other FO, the classical example being the dissociation of the hydrogen molecule into two hydrogen atoms in which RHF would – completely in error – predict a proton and a hydrogen anion to form.

The failure to allow for equivalent, degenerate electronic configurations is a fundamental limitation for any single determinant wave function and in pursuit of exactness the logical conclusion is to use more determinants, permitting other electronic configurations, to describe the wave function for this type of problems. Generally, these wave functions are expressed as a linear combination of Slater determinants

$$\Psi_{tot} = c_0\Psi_0 + c_S\Psi_S + c_D\Psi_D + c_T\Psi_T \cdots . \tag{2.4.2}$$

The wave functions $\Psi_{0,S,D,T,\ldots}$ of the linear combination are all Slater determinants corresponding to ground state and all singly, doubly, triply (and so on) excited states and the coefficients $c_{0,S,D,T,\ldots}$ serve the dual purpose of weights to the individual wave functions and as a normalisation of the total wave function. When Ψ_0 is set to be Ψ_{HF}, the HF ground state, and $\Psi_{S,D,T,\ldots}$ contain all possible ways to arrange N electrons in M orbitals, the method is called *full Configuration Interaction* (full-CI) which is an exact description of the wave function, provided that the basis set employed is exact. Full-CI includes all correlation energy, dynamic and non-dynamic but suffers from the momentous disadvantage that the amount of determinants in the linear combination quickly become astronomical for larger systems and it is thus of limited practical use for the applied quantum chemist. Generally though, it turns out that only some of the determinants have significant weight and good approximations can be made by including only a few determinants. This is the foundation of a number of methods which are of practical use even for larger systems.

There is one way to describe at least the dynamical correlation in a one-electron formalism though: Density Functional Theory (DFT), which differs from wave mechanics in a fundamental way in that it uses the electron density $\rho(\mathbf{r})$, rather than the wave function, as the fundamental argument to describe properties of electronic systems.

2.5 Density functional theory

The difference between a functional and a function is that, whereas a function produces a value depending on its variables, a functional generates a value depending on a function. The functional can accordingly be seen as a function of a function – which depends on variables. The area under a curve in a diagram is then a functional while the curve – the argument of the functional – is defined by a function of a variable. The notation used below follows a common standard where a functional is shown in capital italic letters with the argument, that is to say the function, within square brackets.

Modern DFT starts with the seminal theorems by Hohenberg and Kohn[20] showing that the energy of a system in its electronic ground state is a unique functional of the electron density. The Hohenberg-Kohn theorems were not the fruit of immaculate conception however, but rather built on ideas and concepts developed by Thomas, Fermi and Dirac some thirty years before, which is the subject of the next section.

2.5.1 Humble beginnings: The Thomas-Fermi model

Until 1964, when Hohenberg and Kohn presented their seminal paper proving that the electronic energy of a system is a unique functional of the electronic density, DFT only had the status of a model - and a severely limited one as such. The most notable shortcoming of the simple Thomas-Fermi (TF) model[10–12] – from a chemists point of view – is that it does not predict molecular bonds. The TF model, especially the augmented theory (TFD) subsequently presented by Dirac[13] which includes exchange effects, nevertheless serves as a foundation for present days' more elaborate theories and therefore merits a short account.

The model originates from a statistical mechanics treatment of negative fermion particles in a uniformly distributed positive background whose purpose is to maintain charge neutrality. Space is divided into many small cubes with sidelength l and volume $\Delta V = l^3$, each containing a different, fixed amount of electrons ΔN. Furthermore the electrons are assumed to behave as independent fermions, that is to say there is no interaction between the electrons, with the cells independent of one another. That is, space is divided into a lattice of three-dimensional infinite wells for which

the energy levels are given by

$$\begin{aligned}\varepsilon\left(n_x,n_y,n_z\right) &= \frac{h^2}{8ml^2}\left(n_x^2+n_y^2+n_z^2\right)\\ &= \frac{h^2}{8ml^2}R^2, \qquad\qquad n_x,n_y,n_z = 1,2,3,\ldots.\end{aligned} \tag{2.5.1}$$

For higher quantum numbers the number of energy eigenstates, $\phi(\varepsilon)$, with energy less than ε is very well approximated by the volume of an octant with radius R in the (n_x,n_y,n_z)-space. That is

$$\phi(\varepsilon) = \frac{1}{8}\left(\frac{4\pi R^3}{3}\right) = \frac{\pi}{6}\left(\frac{8ml^2\varepsilon}{h^2}\right)^{3/2}. \tag{2.5.2}$$

The density of states, $g(\varepsilon)$ at energy ε, between ε and $\varepsilon+\delta\varepsilon$ can now be obtained through

$$\begin{aligned}g(\varepsilon)\Delta\varepsilon &= \phi(\varepsilon+\delta\varepsilon)-\phi(\varepsilon)\\ &= \frac{\pi}{4}\left(\frac{8ml^2}{h^2}\right)^{3/2}\varepsilon^{1/2}\delta\varepsilon + O\left((\delta\varepsilon)^2\right),\end{aligned} \tag{2.5.3}$$

under the condition that $\frac{\Delta\varepsilon}{\varepsilon} \ll 1$. The total energy of the cell can be calculated as the expectation value of the density of states multiplied by the probability of the state being occupied, which is given by the Fermi-Dirac distribution

$$f(\varepsilon) = \frac{1}{1+e^{\beta(\varepsilon-\mu_0)}}, \qquad \beta = \frac{1}{k_B T}. \tag{2.5.4}$$

The Fermi-Dirac distribution becomes a step function as $\beta\to\infty$, that is as $T\to 0$, meaning that for certain values of ε, $\varepsilon_F < \mu_0$, all states are occupied and consequently for all $\varepsilon_F > \mu_0$ all states are unoccupied. Here, μ_0 denotes the zero temperature limit of the chemical potential, the energy cost of adding or subtracting an electron to the system at 0 K. The expectation value thus becomes:

$$\begin{aligned}\langle E_{cell}\rangle &= 2\int \varepsilon f(\varepsilon)g(\varepsilon)\mathrm{d}\varepsilon = 4\pi\left(\frac{2m}{h^2}\right)^{3/2} l^3\int_0^{\varepsilon_F}\varepsilon^{3/2}\mathrm{d}\varepsilon\\ &= \frac{8\pi}{5}\left(\frac{2m}{h^2}\right)^{3/2} l^3\varepsilon_F^{5/2}.\end{aligned} \tag{2.5.5}$$

The factor two appears due to the doubly occupied levels by an α and a β spin electron.

In order to make a connection between the electronic energy of a cell and the electron density the expectation value of the number of electrons of the cell is calculated as

$$\langle N_{cell}\rangle = 2\int_0^{\varepsilon_F} f(\varepsilon)g(\varepsilon)\mathrm{d}\varepsilon = \frac{8\pi}{3}\left(\frac{2m}{h^2}\right)^{3/2} l^3\varepsilon_F^{3/2}, \tag{2.5.6}$$

which, inserted into Eq. (2.5.5) in turn gives

$$\begin{aligned}\langle E_{cell}\rangle &= \frac{3}{5}\langle N_{cell}\rangle \varepsilon_F = \frac{3h^2}{10m}\left(\frac{3}{8\pi}\right)^{2/3} l^3 \left(\frac{\langle N_{cell}\rangle}{l^3}\right)^{5/3} \\ &= \frac{3h^2}{10m}\left(\frac{3}{8\pi}\right)^{2/3} \Delta V \rho^{5/3}. \end{aligned} \tag{2.5.7}$$

In the last step $\Delta V = l^3$ and $\rho = \langle N_{cell}\rangle / \Delta V$ has been used. Summation of the energy contribution of all cells then yield the total energy of the system. In the limit when $\Delta V \to 0$ this can be done by integration, assuming that ρ is finite, and we obtain

$$T_{TF}\left[\rho(\mathbf{r})\right] = C_F \int \rho^{5/3}(\mathbf{r}) \mathrm{d}\mathbf{r}, \qquad C_F = \frac{3}{10}\left(3\pi^2\right)^{2/3}. \tag{2.5.8}$$

This is the famous Thomas-Fermi kinetic energy functional, which will later be encountered in the LDA (Local Density Approximation) functional which, as was briefly mentioned in the beginning of this section, provides the foundation of modern density functionals.

The most obvious flaw in this model, conceptually, is that the electrons are treated as an ideal gas with no interactions between them or between the lattice cells – a gross simplification considering the long-range interaction between elementary charges. However, this model has historically enjoyed considerable success in certain applications, notably some types of solid state systems, where the underlying assumptions of the model are close to the actual situation encountered, as it were close to uniform background charge and low free electron density.

Neglecting correlation and exchange effects between electrons the total energy of an electronic system can now be written

$$\begin{aligned} E_{TF}\left[\rho(\mathbf{r})\right] &= C_F \int \rho^{5/3}(\mathbf{r}) \mathrm{d}\mathbf{r} - Z \int \frac{\rho(\mathbf{r})}{\mathbf{r}} \mathrm{d}\mathbf{r} + \frac{1}{2} \iint \frac{\rho(\mathbf{r}_1)\rho(\mathbf{r}_2)}{|\mathbf{r}_1 - \mathbf{r}_2|} \mathrm{d}\mathbf{r}_1 \mathrm{d}\mathbf{r}_2 \\ &= T_{TF} + V_{ne} + V_{ee}, \end{aligned} \tag{2.5.9}$$

in which the second term describes the electronic Coulomb interaction with a fixed external field and the third term describes the Coulomb electron-electron repulsion.

The lack of non-classical effects in TF theory was subsequently addressed by Dirac, and a very brief outline of this contribution will be given here. In HF theory for a non-degenerate, closed-shell ground state, the energy of an electronic system – in functional form – is given by:

$$\begin{aligned} E_{HF}\left[\rho_1\right] &= \int \left[-\frac{1}{2}\nabla_1^2 \rho_1\left(\mathbf{r}_1, \mathbf{r}_2\right)\right]_{\mathbf{r}_2 = \mathbf{r}_1} \mathrm{d}\mathbf{r}_1 + \int \rho(\mathbf{r}) v(\mathbf{r}) \mathrm{d}\mathbf{r} \\ &\quad + J\left[\rho\right] - \frac{1}{4} \iint \frac{\rho_1^2(\mathbf{r}_1, \mathbf{r}_2)}{r_{12}} \mathrm{d}\mathbf{r}_1 \mathrm{d}\mathbf{r}_2, \end{aligned} \tag{2.5.10}$$

where $\rho_1(\mathbf{r}_1,\mathbf{r}_2)$ is the first order spinless density matrix and $v(\mathbf{r})$ of the second term is the external field experienced by the electrons. Comparing this with (2.5.9) we can make the identification

$$V_{ee} = J\left[\rho\right] - K\left[\rho\right], \tag{2.5.11}$$

in which $K\left[\rho\right]$ is the HF exchange-energy functional

$$K\left[\rho\right] = \frac{1}{4}\iint \frac{\left|\rho_1(\mathbf{r}_1,\mathbf{r}_2)\right|^2}{r_{12}}\mathrm{d}\mathbf{r}_1\mathrm{d}\mathbf{r}_2. \tag{2.5.12}$$

It remains to find the density matrix $\rho_1(\mathbf{r}_1,\mathbf{r}_2)$ to obtain an exchange-energy functional from the electron density. In deriving the TF kinetic energy functional the uniform electron gas was modeled as a collection of non-interacting infinite well boxes. Assuming we have a large number of particles – for statistical mechanics arguments to be valid – we can replace the infinite potentials of the boxes by periodic boundary conditions, that is $\psi(x+l) = \psi(x)$. The solution to this problem, cf. particle on a ring, are the orbitals

$$\psi(k_x,k_y,k_z) = \frac{1}{l^{3/2}}e^{i(k_x x + k_y y + k_z z)} = \frac{1}{V^{1/2}}e^{i\mathbf{kr}} \tag{2.5.13}$$

in which

$$k_x = \frac{2\pi}{l}n_x, \quad k_y = \frac{2\pi}{l}n_y, \quad k_z = \frac{2\pi}{l}n_z, \quad n_{x,y,z} = 0,\pm1,\pm2\ldots. \tag{2.5.14}$$

This makes it possible to form a density matrix extending through all space, thereby enabling the expression of the matrix element $\rho_1(\mathbf{r}_1,\mathbf{r}_2)$ as a function of $\rho(\mathbf{r})$ alone (using the change of variables $\mathbf{r} = \frac{1}{2}(\mathbf{r}_1+\mathbf{r}_2)$ and $\mathbf{s} = \mathbf{r}_1 - \mathbf{r}_2$. For a detailed description see, for instance, *Density-Functional Theory of Atoms and Molecules*[15])

$$\rho_1(\mathbf{r}_1,\mathbf{r}_2) = 3\rho(\mathbf{r})\left[\frac{\sin t - t\cos t}{t^3}\right] = \rho_1(\mathbf{r},s), \quad t = k_F(\mathbf{r})s. \tag{2.5.15}$$

in which s appears as the magnitude of $\mathbf{s}$ and $k_F(\mathbf{r}) = \left[3\pi^2\rho(\mathbf{r})\right]^{1/3}$. We are now in a position to formulate Dirac's exchange-energy functional

$$\begin{aligned} K_D &= \frac{1}{4}\iint_{\Omega}\frac{\left|\rho_1(\mathbf{r},s)\right|^2}{s}\mathrm{d}\mathbf{r}\mathrm{d}s \\ &= 9\pi\int\frac{\rho^2(\mathbf{r})\mathrm{d}\mathbf{r}}{k_F^2}\left[\int_0^\infty\frac{(\sin t - t\cos t)^2\mathrm{d}t}{t^5}\right] \\ &= C_x\int\rho^{4/3}(\mathbf{r})\mathrm{d}\mathbf{r}, \quad \text{where} \quad C_x = \frac{3}{4}\left(\frac{3}{\pi}\right)^{1/3}. \end{aligned} \tag{2.5.16}$$

The full energy functional then reads

$$E_{TFD}\left[\rho\right] = C_F \int \rho(\mathbf{r})^{5/3} \mathrm{d}\mathbf{r} + \int \rho(\mathbf{r})\, v(\mathbf{r}) \mathrm{d}\mathbf{r} + J\left[\rho\right] - C_x \int \rho(\mathbf{r})^{4/3} \mathrm{d}\mathbf{r} \quad (2.5.17)$$

Finally we can now behold TFD density functional theory in its full – albeit modest – glory through this inconspicuous expression.

This was the state of the DFT matter until the mid-sixties and the contributions by Hohenberg, Kohn and Sham which elevated the status of DFT above that of a model into a useful tool for electronic structure calculations.

2.5.2 The Hohenberg-Kohn theorems

Density functional theory would never have been more than a model had Hohenberg and Kohn not shown the existence of a unique and universal energy functional of the electronic density of a system.[20] More specifically, Hohenberg and Kohn (HK) proved that, for a given electronic density, there can be no more than one Hamiltonian, meaning that the external potential $v(\mathbf{r})$ of the Hamiltonian can only differ by a constant. In other words, the electronic density of the ground state is exactly determined by the external potential.

The proof is delightfully simple: Suppose there exists two Hamiltonians, $\hat{H}$ and $\hat{H}'$, differing by more than a constant, whose ground state wave functions, Ψ and Ψ', give rise to the identical density $\rho(\mathbf{r})$. The variation principle then dictates that, when $\hat{H}$ operates on Ψ'

$$\begin{aligned} E_0 &< \left\langle \Psi' \middle| \hat{H} \middle| \Psi' \right\rangle = \left\langle \Psi' \middle| \hat{H} + \hat{H}' - \hat{H}' \middle| \Psi' \right\rangle \\ &= \left\langle \Psi' \middle| \hat{H}' \middle| \Psi' \right\rangle + \left\langle \Psi' \middle| \hat{H} - \hat{H}' \middle| \Psi' \right\rangle \\ &= E_0' + \int \rho(\mathbf{r}) \left(v(\mathbf{r}) - v'(\mathbf{r}) \right) \mathrm{d}\mathbf{r}, \end{aligned} \quad (2.5.18)$$

and likewise when $\hat{H}'$ operates on Ψ

$$\begin{aligned} E_0' &< \left\langle \Psi \middle| \hat{H}' \middle| \Psi \right\rangle = \left\langle \Psi \middle| \hat{H}' + \hat{H} - \hat{H} \middle| \Psi \right\rangle \\ &= \left\langle \Psi \middle| \hat{H} \middle| \Psi \right\rangle + \left\langle \Psi \middle| \hat{H}' - \hat{H} \middle| \Psi \right\rangle \\ &= E_0 + \int \rho(\mathbf{r}) \left(v'(\mathbf{r}) - v(\mathbf{r}) \right) \mathrm{d}\mathbf{r}. \end{aligned} \quad (2.5.19)$$

Adding the two expressions Eq. (2.5.18) and Eq. (2.5.19), RHS to RHS and LHS to LHS, yields the contradiction

$$\begin{aligned} & E_0 + E_0' < E_0' + E_0 + \int \rho(\mathbf{r}) \left(v(\mathbf{r}) - v'(\mathbf{r}) \right) \mathrm{d}\mathbf{r} + \int \rho(\mathbf{r}) \left(v'(\mathbf{r}) - v(\mathbf{r}) \right) \mathrm{d}\mathbf{r} \\ & \quad \Leftrightarrow \\ & E_0 + E_0' < E_0' + E_0 + \int \rho(\mathbf{r}) \left[v(\mathbf{r}) - v(\mathbf{r}) + v'(\mathbf{r}) - v'(\mathbf{r}) \right] \mathrm{d}\mathbf{r} \\ & \quad \Leftrightarrow \\ & E_0 + E_0' < E_0' + E_0. \end{aligned} \quad (2.5.20)$$

The sum of two energies can clearly not be less than itself and the proof is complete. The second of the HK theorems proves that there exists a DFT equivalent to the variation principle of wave mechanics and the reasoning is straight forward. Suppose that a well behaved electron density exists which integrates to the correct number of electrons N. In such cases the first theorem proves that there is a wave function corresponding to this density and therefore the following must hold

$$\left\langle \Psi \middle| \hat{H} \middle| \Psi \right\rangle = E \geqslant E_0, \tag{2.5.21}$$

according to the variation principle. The variation principle for DFT is valid in cases where

$$\int \sqrt{\left|\nabla \rho(\mathbf{r})\right|} \mathrm{d}\mathbf{r} < \infty, \quad \int \rho(\mathbf{r}) \mathrm{d}\mathbf{r} = N \quad \text{and} \quad \rho(\mathbf{r}) \geqslant 0, \tag{2.5.22}$$

provided that an anti-symmetric wave function can be constructed from $\rho(\mathbf{r})$. Any density abiding by these requirements which reduces the total electronic energy is a better approximation to the exact density. The theorems unfortunately offer no guide as to how the density should be constructed or to the particular form of the energy functional. The former problem was addressed by Kohn and Sham in 1965.[21]

2.5.3 Kohn-Sham theory

The energy functional mapping a value of the energy from the electron density can be separated in two parts, as in HF theory. One part describes how a system of non-interacting electrons moves in the external potential and the other part describes the electron-electron interactions. This can be expressed as

$$\begin{aligned} E\left[\rho(\mathbf{r})\right] &= T_{TF}\left[\rho(\mathbf{r})\right] + V_{ne}\left[\rho(\mathbf{r})\right] + V_{ee}\left[\rho(\mathbf{r})\right] + \Delta T\left[\rho(\mathbf{r})\right] + \Delta V_{ee}\left[\rho(\mathbf{r})\right] \\ &= E_{TF}\left[\rho(\mathbf{r})\right] + \Delta T\left[\rho(\mathbf{r})\right] + \Delta V_{ee}\left[\rho(\mathbf{r})\right]. \end{aligned} \tag{2.5.23}$$

All terms of the expression have the same electronic density as their argument and the first three terms on the right hand side are one-electron functionals and would, for a system of non-interacting electrons, describe this exactly. The first term, $T_{TF}\left[\rho(\mathbf{r})\right]$, is the kinetic energy functional as obtained from statistical mechanics for a non-interacting electron gas,[10–12] see Section 2.5.1. The second term, $V_{ne}\left[\rho(\mathbf{r})\right]$, expresses the interaction between the nuclei and electron density and $V_{ee}\left[\rho(\mathbf{r})\right]$ is the classical electron-electron repulsion for electronic densities. $\Delta T\left[\rho(\mathbf{r})\right]$ is a correction term to the non-interacting kinetic energy functional $T_{TF}\left[\rho(\mathbf{r})\right]$

of Thomas and Fermi.

$$
\begin{aligned}
T_{TF}\left[\rho(\mathbf{r})\right] &= C_F \int \rho^{5/3}(\mathbf{r})\mathrm{d}\mathbf{r}, \qquad C_F = \frac{3}{10}\left(3\pi^2\right)^{2/3} \\
V_{ne}\left[\rho(\mathbf{r})\right] &= \sum_{k=1}^{M} \int \frac{Z_k}{|\mathbf{r}-\mathbf{R}_k|}\rho(\mathbf{r})\mathrm{d}\mathbf{r} \\
V_{ee}\left[\rho(\mathbf{r})\right] &= \frac{1}{2}\iint \frac{\rho(\mathbf{r}_1)\rho(\mathbf{r}_2)}{|\mathbf{r}_1-\mathbf{r}_2|}\mathrm{d}\mathbf{r}_1\mathrm{d}\mathbf{r}_2.
\end{aligned} \tag{2.5.24}
$$

The two last terms of Eq. (2.5.23) are corrections to the kinetic energy and electron-electron interaction energies needed to account for the errors introduced by assuming a system of non-interacting electrons. These terms are commonly added into a single term, the exchange correlation functional $V_{xc}\left[\rho(\mathbf{r})\right]$.

Within the Kohn-Sham (KS) formalism the assumption is now made that the total density, analogous to the wave function in HF formalism, consists of orbitals, that is

$$
\rho(\mathbf{r}) = \sum_i \left|\phi_i(\mathbf{r})\right|^2, \tag{2.5.25}
$$

and that the functionals in Eq. (2.5.23) are rewritten as a sum of one-electron functionals

$$
\begin{aligned}
E\left[\rho(\mathbf{r})\right] = \sum_i^N \Bigg[&\left\langle \phi_i \right| -\frac{1}{2}\nabla_i^2 \left|\phi_i\right\rangle - \left\langle \phi_i \right| \sum_k^M \frac{Z_k}{|\mathbf{r}_i-\mathbf{R}_k|} \left|\phi_i\right\rangle \Bigg] \\
&+ \sum_i^N \left\langle \phi_i \right| \frac{1}{2}\int \frac{\rho(\mathbf{r}')\mathrm{d}\mathbf{r}'}{|\mathbf{r}_i-\mathbf{r}'|} \left|\phi_i\right\rangle + V_{xc}\left[\rho(\mathbf{r})\right].
\end{aligned} \tag{2.5.26}
$$

The correction terms in the energy expression Eq. (2.5.23) are represented here by the exchange-correlation term $V_{xc}\left[\rho(\mathbf{r})\right]$. Note, that if the exact form of the exchange-correlation term was known, DFT would be an *exact method*, just like full-CI. Alas it is not, and even if it was known, it is unlikely that the evaluation of it would prove easier than other methods including electron correlation. The exchange-correlation functional is usually split in two parts, an exchange and a correlation part.

$$
V_{xc}\left[\rho(\mathbf{r})\right] = V_x\left[\rho(\mathbf{r})\right] + V_c\left[\rho(\mathbf{r})\right]. \tag{2.5.27}
$$

Since $E_{tot}\left[\rho(\mathbf{r})\right]$ can be written as a sum of one-electron functionals, the same method as in HF theory can be applied to form a DFT equivalent to the HF equations, the Kohn-Sham equations

$$
\begin{aligned}
&\hat{\mathbf{h}}_{KS}\phi_i = \varepsilon_i\phi_i \\
&\hat{\mathbf{h}}_{KS} = -\frac{1}{2}\nabla^2 + V_{ne}(\mathbf{r}) + \int \frac{\rho\left(\mathbf{r}'\right)}{|\mathbf{r}-\mathbf{r}'|} + V_{xc}(\mathbf{r}),
\end{aligned} \tag{2.5.28}
$$

where $\hat{\mathbf{h}}_{KS}$ is the DFT equivalent of the Fock operator in wave mechanics. In practice, the solution to these equations is found using the same approach as in the solution to the Roothaan equations in HF theory.

2.5.4 Exchange-correlation functionals

Without going in to details as to how the exchange-correlation functionals are constructed, there have historically been two main schemes at different levels of approximation, the second one being a development of the first. The earliest functionals were derived using the assumption that the electron density in some point **r** *locally* could be treated as a uniform electron gas and is called Local Density Approximation (LDA) or, LSDA for open shell systems.[22]

The second way to formulate the functionals emerged as a correction to the LDA in which the correction term, which is a function of the density gradient in point **r**, is added to the LDA functional. In spirit this resembles a Taylor expansion of $E_{xc}\left[\rho(\mathbf{r})\right]$ and these functionals are called Gradient Corrected (GC) or Generalised Gradient Approximation (GGA) functionals.

For molecular systems however, it is most common today that another type of functional is utilised where a linear combination of the exact exchange contribution (from HF) and a DFT exchange-correlation functional are employed. For instance, the Becke88[23] (B88) three parameter exchange-correlation functional[24] (B3) has the following appearance

$$E_{xc}^{B3} = (1-a)E_x^{LSDA} + aE_x^{exact} + b\Delta E_x^{B88} + E_c^{LSDA} + c\Delta E_c^{GGA}, \tag{2.5.29}$$

where the a, b and c parameters determine the contribution from the different components and whose values are determined by fitting to experimental data. The functional terms on the right hand side are, in order, exchange from LSDA (or LDA for a closed shell system), exact exchange from HF, the B88 GGA exchange correction, the LSDA correlation functional and finally a GGA correlation correction of free choice. Although the choice of last term is free, benchmarks on well characterised model systems[25] (test sets) suggest that the best all-round GGA correlation functional correction to combine with B3 is the Lee, Yang and Parr (LYP) correlation functional[26] for most systems yielding the B3LYP[27] exchange-correlation functional:

$$E_{xc}^{B3} = (1-a)E_x^{LSDA} + aE_x^{exact} + b\Delta E_x^{B88} + (1-c)E_c^{LSDA} + c\Delta E_c^{LYP}. \tag{2.5.30}$$

The slightly different form of this functional compared to Eq. (2.5.29) is due to the lack of an LDA component in the LYP correlation functional.

2.6 Comparison of wave function methods and DFT

DFT has a conceptual advantage compared to wave function methods (with the exception of full-CI) in that it is an exact method under the condition that the exact form of the exchange-correlation functional is used. A conceptual disadvantage of DFT is that, since the exact exchange-correlation functional is not known, there is no gradual way to improve the computed

electronic structure by inclusion of more electronic configurations in the total wave function (or density), as there is in wave function methods. Furthermore, in DFT one can not be certain that the variation principle holds as you can in wave mechanics. The HK theorem does infer that to be the case, but only under the condition that the energy functional is fully known, which it is not, as previously mentioned.

The Kohn-Sham orbitals of DFT do not have the same physical meaning as the HF orbitals, but often in practice they show good agreement with experimental observations. However, the meaning of the virtual orbitals is uncertain and as a consequence so is the validity Koopman's theorem, stating that a species ionisation potential is equal to the negative of the highest occupied molecular orbital energy. Therefore caution is due when studying ionisation energies and electron affinities using DFT.

Within a one determinant description of electronic systems though, DFT has an advantage of including correlation (dynamic) in the formalism and the precision of a calculation in comparison to the computational effort required (CPU time) to achieve it, speaks heavily in favour of DFT in comparison to wave function methods.

The formal scaling of DFT is, like in HF theory, M^4 (where M is the number of basis functions used) but can by computational methods be reduced to M^3. DFT thus have a small advantage on HF and consequently enjoys a much larger advantage on wave function methods including correlation using many Slater determinants.

2.7 From quantum to chemistry

This far in the presentation of quantum chemistry the emphasis has been put on the theoretical underpinnings permitting the study of chemical reactions computationally. It is mentioned in the beginning of this chapter that knowing the electronic structure of a molecule or atom in principle allow all chemical properties of the species of interest to be computed. So how is this done in practise when studying a chemical reaction by means of quantum chemistry on a computer?

For our purposes, a chemical reaction can be defined as a rearrangement process of electrons and nuclei. In most cases of interest the nuclei and electrons are rearranged into something distinguishably different from the initial species, which is not to say that this is true of all chemical reactions. In any case, the gist of it is that bonds are broken and formed. There can be several causes for such events, commonly molecules colliding through thermal motions or electronic excitations due to electromagnetic irradiation.

A chemical reaction can be modeled on a computer in all but a few cases, since the wave function or electronic density of almost any configuration

of nuclei can be obtained. For instance via methods such as those outlined in the preceding sections. Provided the number and species of particles are constant, the energies of any assemblage of these nuclei and electrons are comparable entities[†]. Therefore, because all chemical reactions are mass conserving, the energies of reactants, products and any intermediate structure are all confined to the same "Potential Energy Surface"[‡] (PES), an energy landscape. Just like countryside landscapes, the PES features a counterpart to hills, crests, depressions and passes, which all correspond to a unique geometric configuration of the nuclei.

Using the landscape likeness in the context of chemistry, a reaction starts in a depression traversing a hillside through a pass – or series of passes – down a slope to another depression. In more general, mathematical terms a reaction starts in a minimum, moves against the gradient, passing a saddle point of some order and then follows the gradient to another minimum. This sequential traversing of the PES defines a reaction coordinate which usually bear little likeness to the common notion of a coordinate as a direction or vector. Rather is an abstract concept which *may* coincide with the common definition.

In quantum chemistry, knowing the reaction coordinate is imperative when studying a reaction, since in order to quantitatively assess the validity of a potential reaction mechanism, the route from reactants to products must be ascertained. There are of course an infinite amount of conceivable routes but what is most commonly sought is the most likely route, following the path of least resistance. The crux lies in finding the molecular geometry of the transition state (TS), a saddle point on the PES, which connects the reactant and product geometries.

One guide to finding a TS is offered by the Hammond-Leffler postulate,[28,29] saying that states close in energy have similar geometry, which means that for an endergonic reaction the TS should resemble the product more that the reactant while the reverse would be true for an exergonic reaction. There are a number of techniques to find TSs at various levels of automation. For instance, the simplest systematic approach would be a linear interpolation between the geometries of the reactants and products. Keeping the Hammond-Leffler postulate in mind, linear geometry interpolation would consequently be suitable for thermoneutral reactions and successively less suitable the more ender- or exergonic the reaction becomes. Whichever situation, an unequivocal property of the PES in the vicinity of a TS is that at least one vibrational mode will have negative curvature. Following the negative curvature upward in energy, a saddle point is eventually reached which is the TS geometry.

[†]Comparable in the apples to apples sense.

[‡]A PES is a *hypersurface* in all but diatomic molecules.

Regardless how reactant, product and TS geometries are found, their status must be verified. This is accomplished by standard methods of multi dimensional analysis. All of the mentioned states are stationary in the sense that the gradient of the energy with respect to nuclear coordinates is zero

$$\overrightarrow{\nabla} E = \left(\frac{\partial E}{\partial R_{1x}}, \frac{\partial E}{\partial R_{1y}}, \frac{\partial E}{\partial R_{1z}}, \ldots, \frac{\partial E}{\partial R_{Mx}}, \frac{\partial E}{\partial R_{My}}, \frac{\partial E}{\partial R_{Mz}} \right)^T = \overrightarrow{0}. \tag{2.7.1}$$

In addition, a minimum of the PES must be positive definite, that is the determinant of the Hessian matrix

$$\mathbf{H}(E) = \left(\overrightarrow{\nabla} E \right) \left(\overrightarrow{\nabla} E \right)^T = \begin{pmatrix} \frac{\partial^2 E}{\partial R_{1x}^2} & \frac{\partial^2 E}{\partial R_{1x} \partial R_{1y}} & \cdots & \frac{\partial^2 E}{\partial R_{1x} \partial R_{Mz}} \\ \frac{\partial^2 E}{\partial R_{1y} \partial R_{1x}} & \frac{\partial^2 E}{\partial R_{1y}^2} & \cdots & \frac{\partial^2 E}{\partial R_{1y} \partial R_{Mz}} \\ \vdots & \vdots & \ddots & \vdots \\ \frac{\partial^2 E}{\partial R_{Mz} \partial R_{1x}} & \frac{\partial^2 E}{\partial R_{Mz} \partial R_{1y}} & \cdots & \frac{\partial^2 E}{\partial R_{Mz}^2} \end{pmatrix}, \tag{2.7.2}$$

must have only non-negative eigenvalues while a saddle point of first order has one negative eigenvalue. The vibrational modes of the molecule are the eigenvectors of the Hessian. Following the eigenvector corresponding to the negative eigenvalue at a TS geometry in both directions should end up in local minimum, hopefully the reactants and products.

2.8 Solvent models in quantum chemistry

When studying chemical reactions in the condensed phase, effects of the solvent media can not be disregarded, and hence there is a need for an accurate model which takes these effects into account and provides a quantitative treatment of the solvent influence on the reaction. Broadly, the solvent models used in quantum chemistry can be divided in two categories:

- Discrete models, where a number of explicit water molecules are included in the calculations. This approach has the advantage of capturing phenomena where the solvent play an integral part in the reaction studied, *e.g.* transient charge transfers between the solute and solvent. The drawback is the increase in system size and the loss of average effects of solvation.
- Continuum models, in which the solvent media is treated as a featureless continuum with the sole property of providing polarisation charges that mimic the average behaviour of the particular solvent of interest. In cases where specific solute-solvent interactions are of no consequence to the chemistry of the system, continuum models provide a computationally efficient means to model the influence of the solvent.

Of course, any combination of the two approaches is possible and may indeed be required to faithfully model the system under study. The discrete model will not be discussed further and the attention is instead turned to the continuum models, specifically the Polarisable Continuum Model (PCM).

2.8.1 The PCM method

In the PCM[30,31] solvation model the bulk of the solvent is modelled as an infinitely large, continuous dielectric medium. In this medium a cavity is created approximating the shape of the solute so as to accommodate the species under study. The cavity is created by interlocking spheres, each sphere centered on a nucleus of the solute. Overlapping parts of the spheres are discarded and a solvent accessible surface is computed. This surface is then subdivided into surface elements (facets) called tesserae.

Quantitatively, the solute-solvent interactions can be described as a perturbation to the gas phase Hamiltonian (Eq. (2.1.2)), here denoted $\hat{H}_0$, as

$$\hat{H} = \hat{H}_0 + V_{int}. \tag{2.8.1}$$

The perturbation V_{int} is a sum of three distinct types of interactions

$$V_{int} = V_{el} + V_{ster} + V_{disp}, \tag{2.8.2}$$

where the sterical and dispersion parts, V_{ster} and V_{disp}, can be calculated outside of the SCF procedure to reduce the computational cost. V_{el} is a potential created as a response to the solute's electrostatic potential at the surface of the cavity. It has been shown that V_{el} can be expressed in terms of an "apparent charge density" σ appearing on the cavity surface and this forms the basis of this method. The charge density σ is assumed to be constant on each tesserae which allows V_{el} to be expressed as a sum of point charges q_i placed in the centre of the T number of tesserae:

$$V_{el}(\mathbf{r}) = \sum_{i=1}^{T} \frac{q_i}{|\mathbf{r} - \mathbf{r}_i|}. \tag{2.8.3}$$

In recent implementations of PCM, the point charges depend on the electrostatic potential of the solute at the cavity surface and also by the other point charges. This means that a set of coupled linear equations, equal to the number of point charges, must be solved in every SCF cycle to determine the values of the point charges. The system to solve then is

$$\mathbf{Dq} = -\mathbf{b}_{sol}. \tag{2.8.4}$$

Here $\mathbf{q}$ is a vector containing the point charges; $\mathbf{b}_{sol}$ is the vector containing the solute's electrostatic potential. The matrix $\mathbf{D}$ depends on the dielectric constant of the solvent media and geometrical parameters of the cavity shape. Solving Eq. (2.8.4) allows us to define the perturbation operator V_{el}, and consequently V_{int}, and solve the Schrödinger equation.

3. The chemistry of the anti-tumour drug cisplatin

The anti-tumour drug cisplatin has been the subject of substantial scrutiny. The interest was sparked by the serendipitous discovery of its cytostatic activity, and subsequent publication in 1965, by Barnett Rosenberg *et al.*[32,33] and a plethora of articles has been published on the subject. Nevertheless, many aspects of its mechanism of action are still veiled to us, providing an impetus for further research.

The allure of cisplatin as a research topic is perhaps best understood in terms of its extraordinary efficacy at killing some types of cancer while failing at other. For instance, cisplatin cures testicular cancer with upward of ~90% success rate,[1] when promptly diagnosed. Obviously it is nearly impossible, to improve upon such a figure, but it only pertains to a limited number of cancer types. The reasons for cisplatin resistance in some tumours are complex and multiple factors have been indicated to contribute. The issue of cisplatin resistance will be left at that in this chapter, since it is out of scope for the current work, not because it is uninteresting. Quite the contrary.

Circumventing the cellular mechanisms of resistance is naturally an enticing prospect, given the proven potency of cisplatin against susceptible tumours. However, despite the great humanitarian interest, commercial incentive and the consequential investments made in research, few substantial improvements to cisplatin have been found with respect to broadening the spectrum of treatable cancer types or enhancing its chemotherapeutic potency.

Recently, researchers have therefore taken radical departures from the established formula for anti-cancer activity in Platinum compounds by investigating poly-nuclear complexes, trans arranged complexes and octahedral Platinum species[34–39] in an attempt to avoid mechanisms of cellular resistance, while retaining the DNA binding properties of the parent compound. This certainly does not render the use of cisplatin as a model system obsolete however, since in these novel compounds, the DNA binding "unit" is still a square planar Platinum moiety, which in all likelihood shares many mechanistic aspects of its DNA interactions with cisplatin.

Many aspects of the cisplatin-DNA interaction and also the activation reactions prior to binding are well suited for studies employing the tools of quantum chemistry. While quantum chemistry may not be the best

drug discovery tool in itself due to hardware and software constraints [†], the basic knowledge acquired in this manner should aid the development of novel cisplatin-based cancer drugs. Quantum chemical studies of cisplatin's bonding to DNA and the reactions preceding it are the focus of this chapter.

3.1 Chemical properties of cisplatin

Cisplatin is a small, square planar inorganic compound with a Pt(II) ion in the centre of the square coordinating two ammine and two chloride ligands to the corners of the square in a cis conformation (figure 3.1). Cisplatin's chemical formula, $Pt[NH_3]_2[Cl]_2$, was determined in 1845[40] by Michel Peyrone from whom the older, but occasionally still encountered name of the compound, "Peyrone's chloride", was taken.

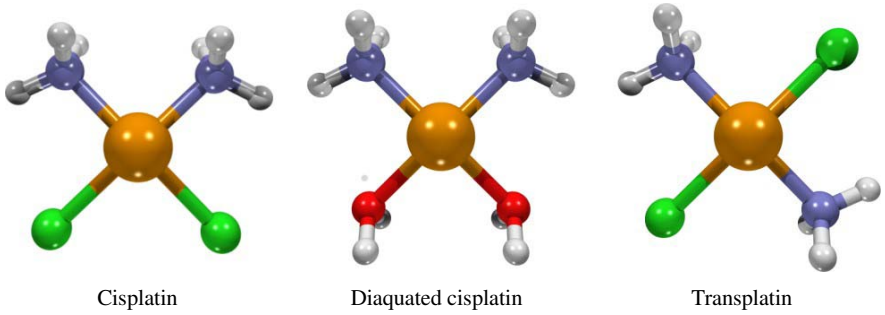

Figure 3.1: Images of cisplatin, diaquated cisplatin and cisplatin's geometrical isomer transplatin.

The principal features of cisplatin's structure were published in 1893[41] by Alfred Werner, a giant in coordination chemistry, whose work on chemical valence and structural chemistry later on earned him a Nobel prize. In that ground breaking publication Werner also presented the first distinction between cisplatin and geometric isomer transplatin, which binds to DNA but does not display any deleterious effects on cancer tumours.

The underlying explanation to cisplatin's square planar geometry was not given until the next century however, through the work of Bethe and van Vleck on Crystal Field Theory (CFT),[42,43] which provides a qualitatively valid quantum chemical explanation for the square planar structure as well as other common structures of coordination compounds, for instance the six-coordinated octahedral geometry.

[†]Neither processors or quantum chemistry algorithms are efficient, or fast, enough to allow testing of the viability of large numbers of semi-random drug candidates, similar to how molecular mechanics/dynamics is used today in drug discovery.

The chemotherapeutic properties of cisplatin were not discovered until the early sixties[44] by physicist-turned-biologist Barnett Rosenberg and co-workers. In an experiment investigating cellular mitosis, inspired by the similarity between the field lines of electric dipoles and the mitotic spindle, an alternating electric current was passed through a culture of *Escherichia Coli*. The working hypothesis was that the similarity of the mitotic spindle and dipolar electric field lines was not just by chance and could possibly be disrupted at some resonance frequency of the current. The experiment in question was only meant to test the equipment before using mammalian cells, since they were fully aware that prokaryotes do not form a mitotic spindle during cell division.

Employing good chemical common sense they used electrodes of Platinum to conduct the current through the solution, since Platinum is chemically inert – or so they thought. The result of the experiment was that the cells started to elongate, growing in filaments, rather than undergoing cell division. Filamentous growth of *E. Coli* is a sign of impeded mitosis by DNA damage.[45,46] The alternating current was eventually ruled out as the direct cause for this and an electrolytic reaction was considered instead. They found that electrolytic reactions did indeed take place, producing many different chemical species. In the end, the hampered cell division was shown to be caused by cisplatin and a few closely related platinum compounds, which had formed at certain frequencies of the current. Cisplatin was subsequently approved by the Food and Drug Administration of USA in 1978 for treatment of genitourinary [†] tumours.

As a side note, it should be mentioned that the respectable age of the coordination chemistry subject is reflected in some legacy nomenclature which may catch the unfamiliar reader off guard. Examples present in this text are ammine (two m's) , aquation and anation. An ammine is an ammonia ligand. Aquation and anation are each others opposite and denote a ligand substitution of an anion by a water molecule for the former and vice versa for the latter.

3.1.1 Crystal field theory and the cisplatin geometry

Cisplatin is a coordination compound. In general, coordination compounds are characterised by having a number of ligands containing lone pair electrons which are *coordinated* toward an empty orbital of a central metal ion, thereby forming a *coordinate covalent bond*. This type of bond is something halfway between purely ionic and covalent bond in terms of stabilisation energy gained by the linear combination of the involved orbitals.

[†] The organ system encompassing the reproductive organs and the urinary system.

A central concept in coordination chemistry is the coordination number, the number of ligands coordinated to the metal ion. The maximum coordination number possible is determined by how many empty valence orbitals are available, which in turn is decided by the valence electronic configuration of the metal ion, its polarisability and the "strength" of the ligands. Strength refers to the magnitude of the energy split induced in the degenerate valence orbitals of the metal ion. A high magnitude split precludes parallell spin electronic configurations, maximising the number of empty orbitals and consequently also the coordination number.

The coordination number is obtained by multiplying the number of empty orbitals by the number of lobes of these orbitals capable of forming σ-symmetric bonds with the ligand lone-pairs. Usually, the ligands form as regular a polyhedron as possible from the coordination number, where the ligands constitute the polyhedron corners. One exception to this rule of thumb is close at hand; cisplatin, in which Platinum(II) has coordination number four but the ligands are square planar rather than the more regular tetrahedral arrangement.

The coordinating Platinum centre of cisplatin is in the 2+ oxidation state and has the d^8 electronic configuration of its valence shell. This is the most commonly encountered oxidation state of Platinum followed by the 4+ oxidation state, Pt(IV). In contrast to the square planar structure of Pt(II) compounds, Pt(IV) forms octahedral ligand complexes due to its d^6 valence shell electronic configuration as explained below.

The structures of transition metal complexes are intimately related to the valence shell electronic configuration of the coordinating metal center. That is, the extent to which the metal d-orbitals are filled. For any given valence configuration there is a corresponding geometric arrangement of

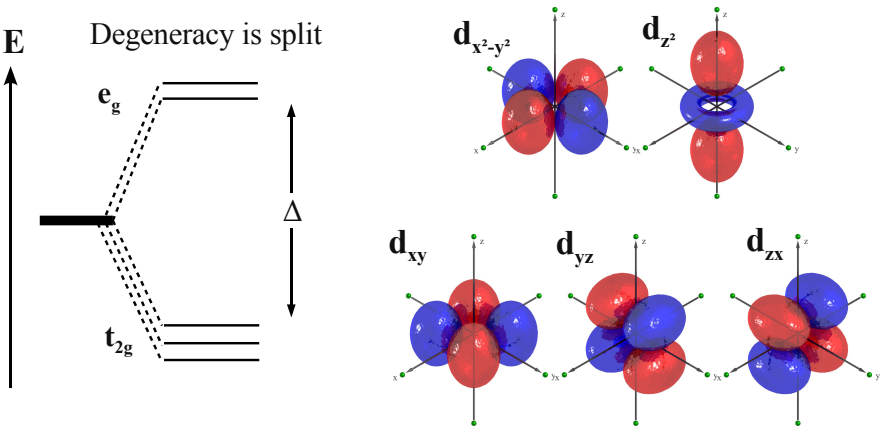

Figure 3.2: Energy split of the d-orbital degeneracy in an octahedral crystal field. The point charges are indicated by green spheres at the end of the axes.

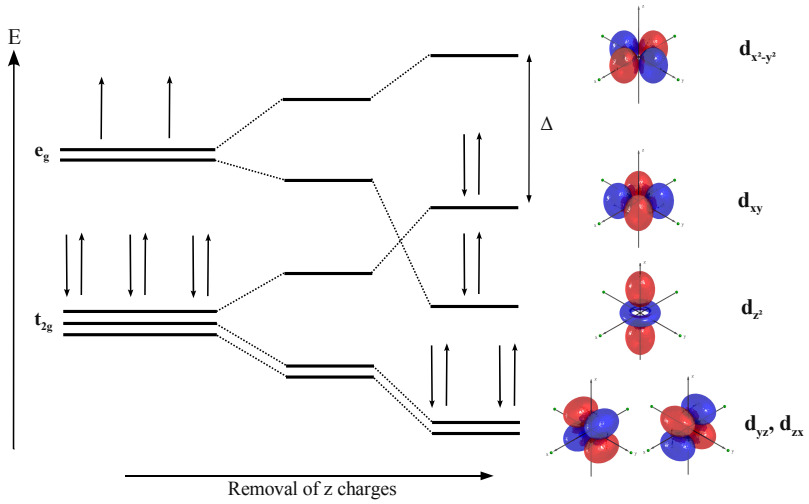

Figure 3.3: Scheme over the broken d-orbital degeneracy in an octahedral crystal field as a function of increasing separation of the z-axis charges. To the right, the orbitals and their relative energy levels corresponding to the electronic configuration of cisplatin (d^8) is shown for a square planar crystal field.

ligands which is the most stable that can be predicted by crystal field theory (CFT).

In CFT the coordinating metal is viewed as a free ion and the ligands are treated as point charges, a source of Coulomb repulsion acting on the electronic density distribution of the d-orbitals. Differently placed point charges around the ionic metal center break the degeneracy of the d-orbitals in specific and unique ways. CFT uses an electrostatic argument alone to explain how the degeneracy of the transition metal d-orbitals is broken depending on the symmetry of the point charge lattice, the crystal field. This is too simplistic a picture to provide better than qualitative predictions and CFT has long since been superseded by Ligand Field Theory and MO theory in that respect. Nevertheless CFT serves as a good vehicle for explaining coordination chemistry.

Due to the spatial distribution of electronic density of the d-orbitals, crystal fields of different symmetry will split the orbital energy levels differently, both in terms of the magnitude of the split, Δ, and the ordering of the d-orbital energy levels. The electronic configuration is then determined in the usual manner following the *aufbau*, or building-up, principle and Hund's rules. In the case of four coordination directions the two prevalent geometrical configurations of ligands in coordination compounds are the tetrahedral and the square planar arrangement, in order of natural occurrence. Using the CFT framework, the square planar arrangement of ligands is obtained as a special case of the octahedral arrangement, shown in figure 3.2,

where the charges of one axis have been infinitely separated as depicted in figure 3.3 which shows the resulting low-spin configuration of cisplatin. For the six-coordinated complexes formed by Pt(IV) it is evident that the octahedral arrangement shown in figure 3.2 puts the six valence electrons in the lowest energy state, making it the preeminent configuration.

The split of energy levels caused by a tetrahedral crystal field is an inversion of the octahedral split, that is, the d-orbitals not aligned to coordinate system axes (d_{xy}, d_{yz}, d_{zx}, the orbitals of e symmetry) are most repelled by the crystal field charges and lie higher in energy than the orbitals aligned to coordinate axes, d_{z^2} and $d_{x^2-y^2}$. The tetrahedral arrangement will consequently put a d^8 valence configured ion in an overall higher energy than the square planar arrangement and is therefore disfavoured.

3.2 Activation of cisplatin

Cisplatin, like most other chemotherapeutic drugs, interacts with DNA to inhibit vital cell processes such as replication and transcription. Cisplatin in its native form is a neutral molecule and hydrolysis of the chloride ions in the blood plasma is suppressed due to the relatively high chloride concentration therein, ~100 mM. This suppression is a necessary requisite for passage through the cell wall by cisplatin, since this passage is most likely passive,[47] and an overall neutral molecule has a much higher rate of passage through the fatty cell wall than a charged species.

Upon entering the cell cytoplasm, the chloride concentration drops to ~20 mM and the cisplatin chlorides are then more susceptible to substitution, shifting the equilibrium toward aquated species, which are more active binding to DNA than the parent compound. The loss of chlorides therefore serves as an activation of the drug. There is no unequivocal evidence as to whether it is the singly or doubly aquated species that bonds to DNA,[48,49] but a majority of the researchers lean towards the singly aquated species.

The aquation reaction of cisplatin is an associative substitution reaction wherein a chloride ligand of cisplatin is replaced by a water molecule in a generalised S_N2 mechanism. Substitution reactions in square planar complexes have been investigated intensively for a number of different compounds including several different metal ions and ligands.[50] The reaction starts with the entering water ligand coordinating to the Platinum ion from one side of the coordination plane, as shown in figure 3.4. The substitution is then likely to proceed via a trigonal bipyramidal transition state[51] to a product complex in which the substituted ligand leaves on the opposite side of the coordination plane. The full aquation of cisplatin involves two

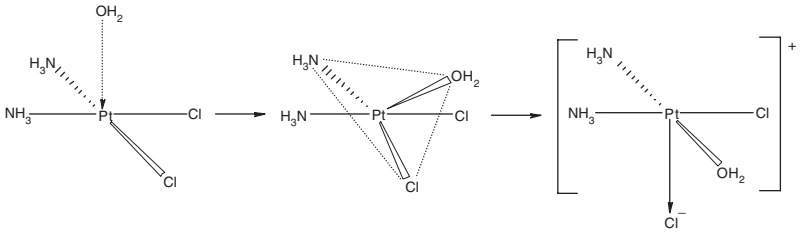

Figure 3.4: Schematic illustration of the theoretical ligand substitution mechanism for cisplatin.

consecutive substitutions of chloride ions by water molecules

$$\textit{cis}\text{-Pt}[NH_3]_2[Cl]_2 + 2H_2O \rightarrow \textit{cis}\text{-Pt}[NH_3]_2[Cl][H_2O]^+ + H_2O + Cl^- \rightarrow$$
$$\textit{cis}\text{-Pt}[NH_3]_2[H_2O]_2^{2+} + 2Cl^-$$

Experimental data pertinent to this reaction include kinetic studies[48,52] and barrier height determinations for the first aquation[53–55] and the chloride anation[56,57] of *cis*-$Pt[NH_3]_2[H_2O]_2^{2+}$ to *cis*-$Pt[NH_3]_2[Cl][H_2O]^+$, and an X-ray structure[58] of cisplatin. One kinetic study[48] indicated that the equilibrium state of aquation of cisplatin in a chloride depleted environment would be the monoaquated species, while analysis of the bonding pattern of cisplatin to DNA using both mono- and diaquated cisplatin suggest the diaquated species to be the activated form.[49]

Despite the considerable resources spent on research of this drug, many questions still remain regarding the mechanism of cisplatin's activation as well as its binding to DNA. Some of these questions, or aspects of them, can be addresses using quantum chemistry: For example, the aforementioned disagreement on which form the drug actually binds to its targets, that is, as *cis*-$Pt[NH_3]_2[Cl][H_2O]^+$, or *cis*-$Pt[NH_3]_2[H_2O]_2^{2+}$. To this end, computational chemistry can be a useful complementary tool, in order to verify or falsify suggested mechanisms, or propose reaction paths of modified drugs. The reaction mechanism of the aquation of cisplatin is studied in paper I.

3.3 Cisplatin interactions with DNA

In the more than three decades passed since the discovery of cisplatins cytotoxicity, the relatively few second generation cisplatin derived drugs, either released to the market or candidate drugs, have generally been active against the same spectrum of tumours as cisplatin, mainly ovarian, testicular, head and neck cancers.[59,60] Two notable improvements to the drug have so far been found however: Firstly, the replacement of cisplatin's chloride ligands with a chelating dicarboxylate group in carboplatin which

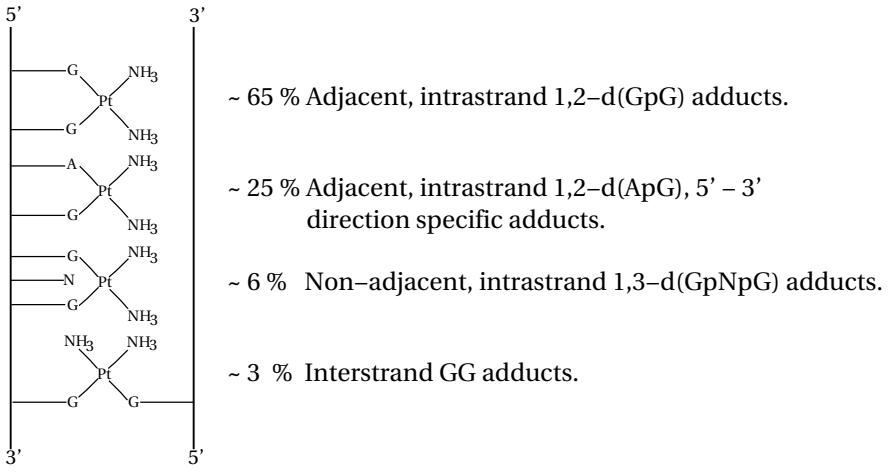

Figure 3.5: Schematic drawing of the different DNA adducts formed by cisplatin. The letter N denotes any base.

resulted in reduced toxicity, thereby permitting higher dosage, less severe side-effects and a reduced need for co-administration of protective drugs. Secondly there has been found one derivative lacking cross-resistance with cisplatin in the case of oxaliplatin which have been approved for the treatment of colorectal cancer.[34,61,62] It is starting to become evident however, that following the established Structure Activity Relationship rules,[2,3] laid out by Cleare and Hoeschele in the seventies, it is not likely that any radically improved drugs will be found, neither with respect to cisplatin cross-resistance nor to highest attainable potency. The latter may not be of primary importance to strive for, as 90 % curing rate is a figure hard to surpass.

Research efforts are now directed toward compounds in direct violaton of most of the established SAR rules, mainly octahedral Pt(IV) species, polynuclear species containing several platinum centres and the rational design of sterically hindered complexes in an attempt to circumvent cellular mechanisms of resistance. In these efforts, quantum chemistry can provide profound understanding of the mechanism of cisplatins action as well as drugs derived from it, since the functional DNA binding group is a square planar Platinum moiety in these drug candidates as well.

The clinical target of cisplatin has in a number of studies been shown to be cellular DNA,[63–65] to which cisplatin forms several different adducts, most notably the intrastrand bifunctional adducts [†] 1,2-d(GpG) at

[†]The nomenclature of these adducts is: 1,2-d({A/G}pG) where "1,2" denotes adjacent purines, "d" means duplex DNA, A and G stands for adenine and guanine respectively while p denotes the phosphate group linker. Adducts of the 1,3-d(GpNpG) type follow the same naming conventions with N meaning *any* base. Interstrand adducts do not follow these conventions and are referred to as "interstrand GG adducts".

~65% and 1,2-d(ApG) at ~25%[66,67] (figure 3.5). These adducts have also been pointed out as the ones correlating to the antitumour properties of cisplatin on account of these not being formed by the clinically inactive geometric isomer transplatin.[68] Other adducts formed are the intrastrand 1,3-d(GpNpG) (N being any base), the interstrand GG adduct, monofunctional adducts to guanine and various DNA-protein adducts. It is worth noting that neither monofunctional adducts to adenine nor interstrand AG adducts have been detected.

The intrastrand adducts and interstrand adducts have principally different arrangements of the purines with respect to the plane formed by the Platinum(II) ion and the carrier ammine ligands. Experimentally determined structures of intrastrand adducts show the O6 atoms of the guanines coordinated toward the same side of the cisplatin plane, whereas interstrand adducts have O6 atoms coordinated on opposite sides of the plane. These arrangements are called the Head-to-Head (HH) and Head-to-Tail (HT) arrangements respectively.

All bifunctional adducts to DNA cause a local unwinding of the DNA helix and a widening of the minor groove, but with significant differences between the intra- and interstrand adducts,[70,71] which are illustrated in figures 3.6 and 3.7. The major platination product, 1,2-d(GpG), induces a kink in the DNA molecule and opens a hydrophobic pocket in the minor groove between the two guanine bases. This kink, and the widened minor groove with the hydrophobic pocket, provide a motif of recognition for a class of protein called "HMG-box proteins",[72–77] so called because they contain a "High Mobility Group" tertiary structure motif common to the HMG group of chromosomal proteins. These proteins provide a wide range

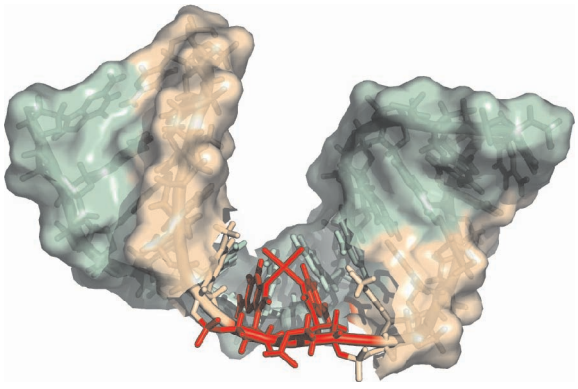

Figure 3.6: The major intrastrand platination product 1,2-d(GpG) determined by NMR spectroscopy in a dodecamer DNA duplex.[69] Highlighted in red is the platination site. The individual DNA strands are coloured wheat and green.

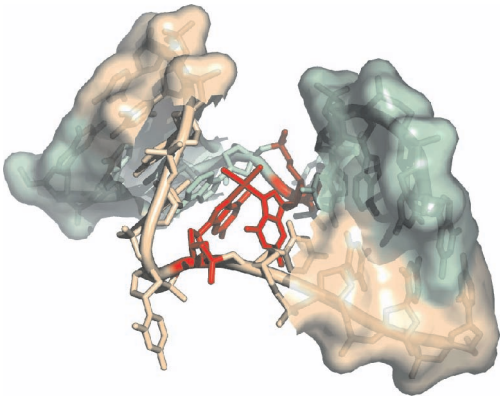

Figure 3.7: X-ray determined structure[71] of the less common interstrand bifunctional platinum GG adduct. The complementary cytosine bases of the adduct guanine bases are expelled out of the DNA helix and extend into the solvent. The colouring follow that of figure 3.6.

of functionality including DNA repair, replication and transcription, all involving recognition of specific DNA sequences.

These proteins can form a ternary complex to the site of the lesion, impeding access to the platinated DNA lesion for the DNA excision repair enzymes of the cell nucleus. The crystal structure of this ternary complex[78] reveals that, besides the common DNA recognition motif of gene regulatory proteins (helix-turn-helix), a phenylalanine side chain was inserted into the hydrophobic pocket created at the site of the lesion, see figure 3.8.

One may ask whether the preference of platination toward G over A is manifested in the chemical differences of the purines, or is due to sterical effects imparted by the surrounding parts of DNA. Furthermore there is an open question about the role of the carrier ligands (NH_3) and especially the need for at least one -NH moiety[79] in the ammine is suggestive of hydrogen bonding. It is for instance well known that the ammine ligand of cisplatin in a dinucleotide 1,2-d(GpG) adduct can form a hydrogen bond to the 5' backbone phosphate group,[80,81] which could provide stabilisation to the induced kink in polynucleotide DNA as well.

3.4 Paper I

In this paper, the full aquation of cisplatin is studied using two models of solvation: One minimal model where the solvation effects are modelled with a continuum solvation model, IEF-PCM,[82–84] and an extended solvation model containing five explicit solvent water molecules in the

first substitution reaction and four explicit water molecules in the second substitution complemented by the IEF-PCM continuum solvation model. There are thus a total of six water molecules present as ligands or solvent molecules at all stages of the aquation process in the large model. The present study aimed to elucidate the most probable aquation state of activated cisplatin in a chloride depleted environment and to find out the effect of the solvation model on the results.

Previous theoretical studies[85,86] have investigated various aspects of cisplatin's activation process, employing different quantum chemical methods. The first study[85] used the Car-Parinello MD method[87,88] (CPMD) to estimate the activation energy barrier of the first aquation of cisplatin at considerable computational expense and obtained a result (~21 kcal/mol) in very good agreement with experimental results (19.5-21.5 kcal/mol), albeit without optimised transition state (TS), reactant complex (RC) or product complex (PC) geometries due to the dynamical nature of the Car-Parinello method. Due to the prohibitive computational cost of CPMD some limiting constraints were put on the cisplatin moiety in order to enforce the ligand substitution within a reasonable time frame and computational effort. Unfortunately this could also introduce a bias in the results which is impossible to assess *a priori* or *a posteriori*. On the other hand it may be argued that the computed barrier height of activation agrees so well with experiment that it alone serves as validation of this computational approach.

The second study[86] employed more traditional quantum chemical methods (DFT) and obtained optimised TSs, RCs and PCs for all stages of the aquation. However, the solvation model used [89,90] (of Onsager ancestry) unfortunately left room for some doubt regarding the accuracy

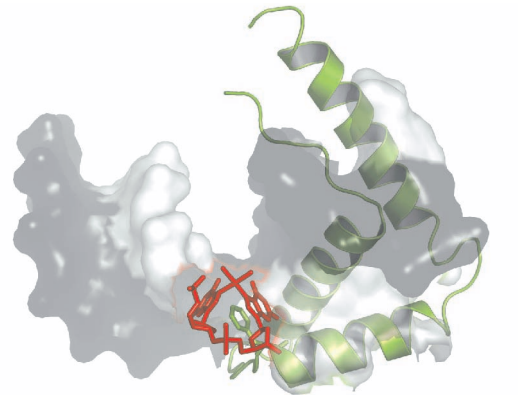

Figure 3.8: X-ray determined structure[78] of an intrastrand 1,2-d(GpG) adduct in a ternary complex with an HMG-box containing protein.

of the results. The Gibbs free energy activation barrier, $\Delta G^{\ddagger}$, for the two aquation reactions was estimated to be 24.1 kcal/mol for the first aquation and 28.6 kcal/mol for the second, while the chloride anation (*cis*-$Pt[NH_3]_2[H_2O]_2^{2+}$ → *cis*-$Pt[NH_3]_2[Cl][H_2O]^{+}$) reaction was found to have a $\Delta G^{\ddagger}$ of 28.5 kcal/mol. When comparing this last barrier to the experimentally determined 16.6 kcal/mol, there is a large discrepancy, most likely due to the solvation model used. Furthermore the study[86] suggested that the second aquation step would be thermoneutral conflicting with kinetic studies of the aquation.

In the present study, the stationary points of the rection path (RC, TS, PC) were located for both the small and the large model using DFT at the B3LYP level of theory. The Effective Core Potential (ECP) basis set LanL2DZ[91–93] was used for the Platinum atom while other atoms were described by the 6-311+G(d,p) basis set.[94,95] Vibrational frequency calculations of the stationary point geometries were performed at the same level of theory and the same basis sets as above to obtain thermodynamical data and to verify minima and first order saddle points. Single point calculations including the IEF-PCM solvation model (water as solvent) were performed on these geometries at the B3LYP/(LanL2DZ + 6-311+G(2d,2p)) level of theory. The diffuse functions of the basis sets were included to properly describe the leaving chloride anions. In the second substitution step the substituted chloride of the first aquation was removed in order to better model a chloride depleted environment, thus enabling a better comparison to experimental data.

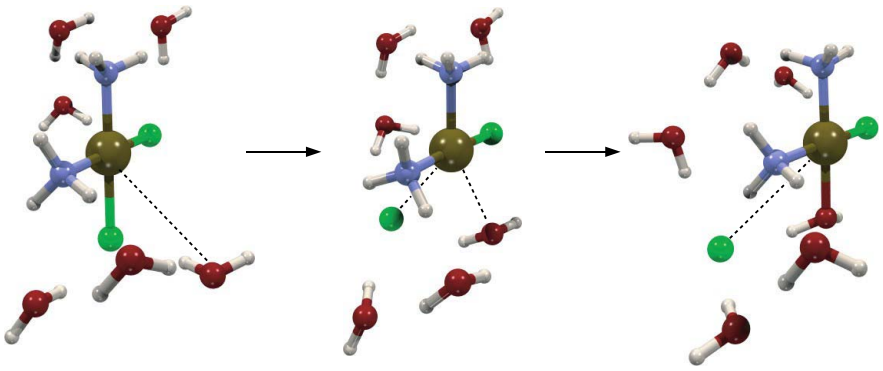

Figure 3.9: Reactants, transition state and product geometries respectively of the first aquation reaction of cisplatin. The extended system including discrete solvation is shown here.

The geometries obtained in the calculations closely follow experimental results and the general theory for ligand substitutions in square planar complexes. An example is shown in figure 3.9 displaying the first aquation of the larger system. All reactant and product complexes are perfectly

planar with metal-ligand bonds of the first reactant complex (corresponding to the crystallographic structure) slightly longer than those determined experimentally. The Pt-Cl bond is here found to be 2.39 Å compared to 2.33 Å experimentally. The Pt-ammine bond was 2.08 Å compared to 2.01 Å in the crystal structure. The slightly longer bonds found in our calculations is not surprising since the DFT functional used is known to produce somewhat too long bonds. The transition states were all trigonal bipyramids with the eqatorial plane of the bipyramid slightly skewed with respect to the bipyramid axis.

The reaction energy profiles of the two models, figure 3.10, show that the energy barriers of the reactions closely follow experimental data. From the data obtained for the large model system, with six water molecules included, it is concluded that the non-bonded waters are important in order to solvate the leaving chloride anions. In absence of this effect, the electrostatic interaction between the negative chloride and the positive platinum is overly pronounced, increasing the barrier heights and magnifying the endergonic character of the two reaction steps.

In comparison with available experimental data, the IEF-PCM calculations on the large model provides a Gibbs energy of activation for the first aquation of 22.8 kcal/mol (experimental value 19.5-21.5 kcal/mol), a nearly thermoneutral first step, a higher barrier for the second aquation ($\Delta G^{\ddagger}$ = 26.7 kcal/mol) and the full aquation process is endergonic by ca. 12.5 kcal/mol. The computed vacuum enthalpies are in good accord with the reported barrier for chloride anation of the fully aquated complex;

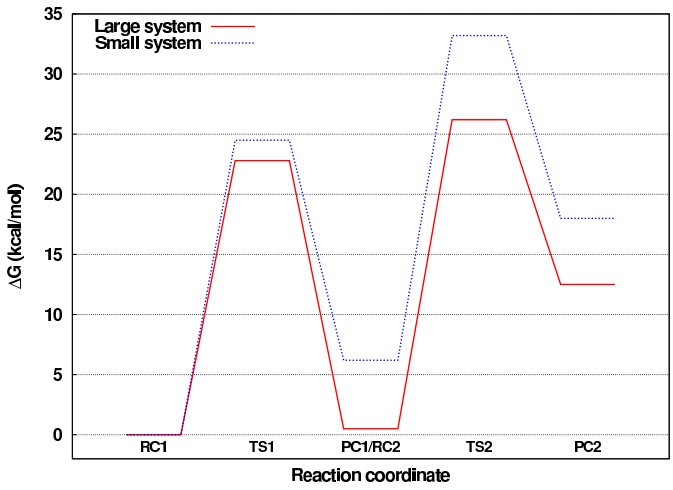

Figure 3.10: Energy profile for the activation reactions of cisplatin using the minimal (dashed line) and the extended (solid line) system. The energies include IEF-PCM solvation model corrections.

computed $\Delta H^{\ddagger}$ = 18.2 kcal/mol vis-à-vis the experimentally measured 16.6 kcal/mol. This can be compared to the computed Gibbs free energies of activation for chloride anation, being ca. 14 kcal/mol.

Considering the energy profile of the larger system, including discrete solvation, it shows that monoaquated cisplatin is thermoneutral with respect to the parent compound and the barrier height of the second aquation is kinetically less favourable by ~4 kcal/mol compared to the first. From these arguments, it is concluded that monoaquated cisplatin should be a preferred form in most chloride depleted environments.

3.5 Paper II

This investigation sought to answer questions regarding the preferential bonding to guanine of cisplatin, both at the initial attack and also for adduct closure. In this work, the reaction energy profiles for the first and second substitution reactions of diaquated cisplatin with adenine and guanine nucleotides are presented. The choice of diaquated cisplatin, rather than monoaquated, as the activated state of cisplatin is motivated by the experimental evidence that the ratio of adducts to DNA formed by diaquated cisplatin closely follow the ratio actually observed[49] *in vivo/vitro*. In the attack of diaquated cisplatin on DNA, the mechanism of the following reactions were investigated:

1. *cis*-$Pt[NH_3]_2[H_2O]_2^{2+} + G \rightarrow$ *cis*-$Pt[NH_3]_2[G][H_2O]^{2+} + H_2O$
2. *cis*-$Pt[NH_3]_2[H_2O]_2^{2+} + A \rightarrow$ *cis*-$Pt[NH_3]_2[A][H_2O]^{2+} + H_2O$
3. *cis*-$Pt[NH_3]_2[G][H_2O]^{2+} + G \rightarrow$ *cis*-$Pt[NH_3]_2[G]_2^{2+} + H_2O$
4. *cis*-$Pt[NH_3]_2[G][H_2O]^{2+} + A \rightarrow$ *cis*-$Pt[NH_3]_2[G][A]^{2+} + H_2O$

The role of initial complex stabilization in governing the system toward observed products is discussed on the basis of the results of the calculations, and a suggestion for the origin of the direction specificity of the 1,2-d(ApG) products is presented.

All calculations were carried out using DFT at the B3LYP level of theory with either the 6-31G(d,p) basis set or the 6-311+G(2d,2p) for non-platinum atoms, where the former basis set was used for geometry optimisations and frequency calculations. The latter basis set was used for single point and counterpoise calculations. The ECP basis set LanL2DZ was used for Platinum. Basis set superposition error was estimated by means of the counterpoise correction and included in the estimates of complexation energy differences between different systems. Solvation energies were obtained by means of IEF-PCM and were included in the final free energy profile of the reactions. All reactions presented were fully characterised in terms of the stationary points along the reaction coordinate. The results obtained in the calculations are compared with established theory on ligand substitution

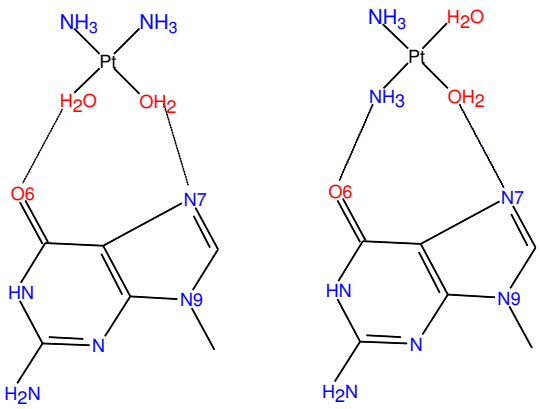

Figure 3.11: Schematic drawing of the two hydrogen-bond patterns between the reactants (shown here: guanine) of the first substitutions found to have associated transition states and product complexes.

in square planar complexes as well as experimental results and previous theoretical work.

In the first substitution, two possible alignments of the purines with respect to the diaquated cisplatin, corresponding to two separate reaction paths, were found and are schematically drawn in figure 3.11. The second substitution employed the two product complexes from the first substitution reaction with guanine (without the substituted water ligand) and either adenine or guanine as second substituents.

The geometries of the stationary points of the first substitution closely agree with previous theoretical work and the established theory for ligand substitution in square planar complexes, some of which are shown in figure 3.12 and figure 3.13. The activation energy barrier for path 1 substitution by guanine (19.5 kcal/mol) closely agrees with both experimental measurements[96] (18.3 kcal/mol) and earlier computational results by others[97] (21.8 kcal/mol). The barriers of the path 2 guanine substitution and path 1 and 2 adenine substitutions were found to be 21.4, 24.8, and 24.0 kcal/mol, respectively. These results are in some discord with comparable results of others[97] where barriers of 25.6, 34.5, and 37.6 kcal/mol were reported. Two main sources of this discrepancy can be distinguished: the differences in basis set employed and the lack of optimized reactant complexes from which to calculate the barrier height in earlier work. All reaction paths are found to be exothermic. The results are graphically presented in figure 3.14.

In a computational study by Baik et al.,[97] the bias of cisplatin toward guanine substitution is concluded to depend on the activation energy barrier alone. Present work instead suggests that cisplatin's preference for substitution with guanine over adenine is governed by the larger thermodynamic stability of guanine's reactant complex in combination with a higher energy

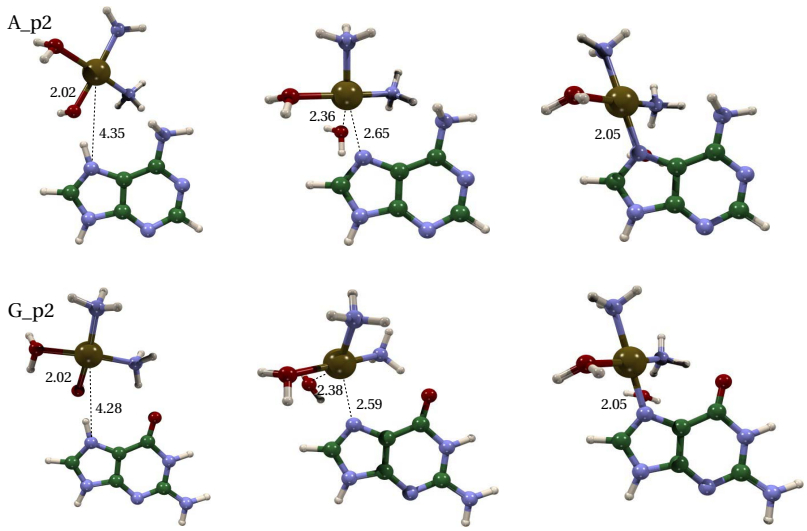

Figure 3.12: First substitution of activated cisplatin and adenine (top row) and guanine (bottom row) following path 2.

of activation for the adenine substitution. The complexation energy difference was calculated to be 7.8 kcal/mol in favor of guanine.

The reactants in the second substitutions are adenine or guanine and cisplatin-guanine product complexes of the first substitution. The aim of studying this substitution was to find the discriminating factors directing the reaction toward the head-to-head (HH) or head-to-tail (HT) configuration of the final product. This would correspond to intra- and interstrand adducts respectively, as found in experimental studies. In addition, this allowed for the origin of the preference for guanine over adenine in the second substitution to be addressed.

Several paths leading to HH and HT product conformations were found for both adenine and guanine, and for the guanine substitution leading to HT configuration, two different paths were located. In general, the HT products stem from reactions starting with the G • p2 product complex as one of the reactants, whereas reactant complexes containing the G • p1 product complex lead to the HH arrangement. The geometries of the stationary points of the second substitutions were found to be in agreement with previous theoretical and experimental studies.

As in the first substitution, the reactions of the second substitution were found to be slightly exothermic, with products in the HT configuration being energetically favored over the HH configuration. This is likely an effect of the smaller steric hindrance of the HT configuration in our model system and does not necessarily represent the situation *in vivo*. The activation energy of the different reaction paths are surprisingly similar

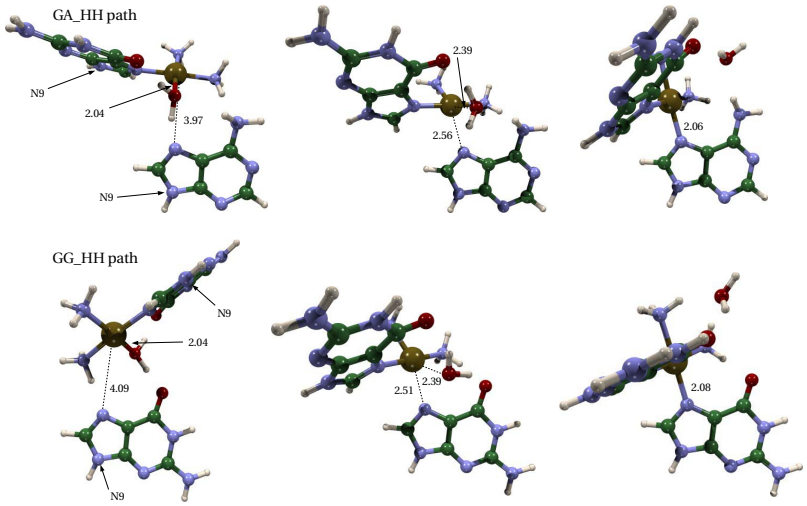

Figure 3.13: Second substitution of activated cisplatin and adenine (top) and guanine (bottom). Both follow a reaction path leading to the Head-to-Head conformation.

(21.1-22.5 kcal/mol) and should thus not constitute the discriminating factor explaining cisplatin's bias toward intrastrand GG adducts. There is good reason to believe the calculated barrier heights to be accurate given that the experimentally determined value for GG adduct closure,[98] 23.4 kcal/mol, agrees well with our computed value for the corresponding reaction (22.5 kcal/ mol). The data obtained for the complexation energy difference between the adenine and guanine reactant complexes of the

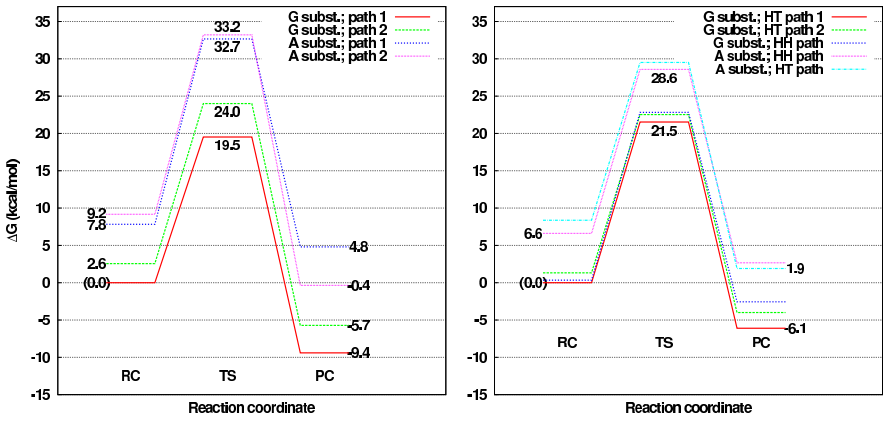

Figure 3.14: Reaction free energy profiles for the first (top) and the second (bottom) purine substitution.

second substitution (6.6 kcal/mol, favoring guanine complex formation) suggest that again the rate of reactant complex formation strongly influences which bifunctional adduct is finally observed.

The observed 5'–3' directionality of 1,2-d(ApG) adducts can be explained by the predominance of initial complex stabilization and binding to guanine. For the second substitution, the DNA geometry allows for binding in the 5'-direction preferentially, and hence 1,2-d(ApG) is formed. Had initial substitution favored adenine, the geometry of DNA had instead biased the system toward 1,2-d(GpA) 5' adducts.

3.6 Paper III

In this follow-up study to paper I, the aquation reaction of promising drug candidate JM118 is studied by means of DFT in a manner very similar to the successful approach used in paper I. Third generation platinum anti-tumour drug JM216, drawn in figure 3.15, is an octahedral compound with the central Platinum(VI) ion coordinating one ammine, one cyclohexylamine and two chloride ligands in a square forming the base of the bipyramid. The axial ligands of the bipyramid are acetate groups.

Platinum(VI) of JM216 is in a low spin electronic configuration and is coordinatively saturated as it coordinates six ligands and it is furthermore quite inert to substitutions. This makes it an excellent candidate for oral administration since it can pass intact through the gastro-intestinal tract. It is generally believed that the Platinum ion of JM216 is then reduced to Pt(II) by either intracellular or extracellular (or both) reducing agents.[99–108] This has the effect that the acetato ligands of JM216 are shed and JM118 is formed *in situ*. JM118 then undergoes activating hydrolysis in the same manner as cisplatin and subsequently binds to DNA.

The hydrolysis of JM118 was studied using three model systems, see figure 3.16. They were:

- A minimal system consisting of only the reacting species, that is JM118 and a water molecule.
- An extended system adding five extra water molecules to provide explicit solvation.
- A system forked off of the extended system after the first substitution where the substituted chloride of the first reaction is kept in the system during the second hydrolysation.

Calculations on these systems were done using the B3LYP DFT functional in conjunction with LanL2DZ ECP basis set for Platinum and 6-311+G(d,p)

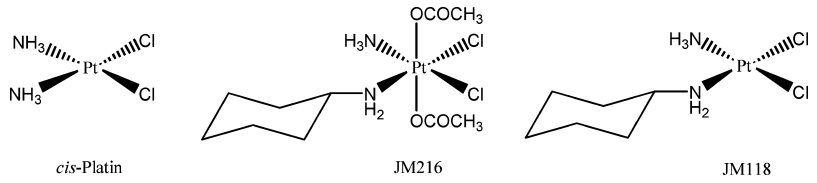

Figure 3.15: Schematic drawings of cisplatin, third generation cisplatin drug candidate JM216 and the reduced, active form JM118.

for remaining atoms in the gas phase optimisations and frequency calculations, supplemented by single point calculations in which basis set 6-311+G(d,p) was exchanged for 6-311++G(3df,2dp). Bulk solvation was modeled using IEF-PCM.

The geometries obtained are in line with previous results for cisplatin and established theory for these substitution reactions.

It is found that explicit as well as implicit solvent effects play a critical role in the energetics of aquation of JM118. Comparisons of the data for the three model systems reveal that the non-bonded water molecules are important to solvate the leaving chloride anions and hence for obtaining accurate reaction profiles. In absence of the explicit solvent effect, the electrostatic interaction between the leaving chloride anion(s) and the remaining platinum complex is overestimated, resulting in higher reaction barriers.

The overall energy profile, shown in figure 3.17 indicate that the doubly aquated species is likely to contribute more to overall binding to DNA in the case of JM118 than for the cisplatin parent compound. Specifically, the second substitution barrier is lower than the first in the larger, more realistic, model systems, making the second chloride kinetically easier to remove than the first. In addition and in line with experimental data for related systems, the computed free energies suggest that JM118 will undergo slower hydrolysis than cisplatin. This has implications for the action and reactivity of the prodrug JM216.

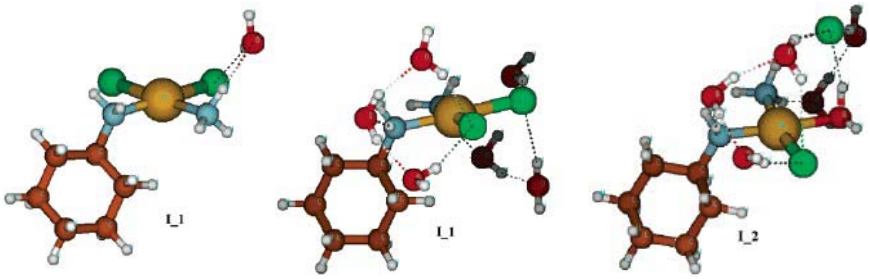

Figure 3.16: The model systems used in the JM118 aquation study.

The slower hydrolysis caused by the addition of the cyclohexylamine group will assist the drug in undergoing initial reduction to JM118 prior to any hydrolysis.

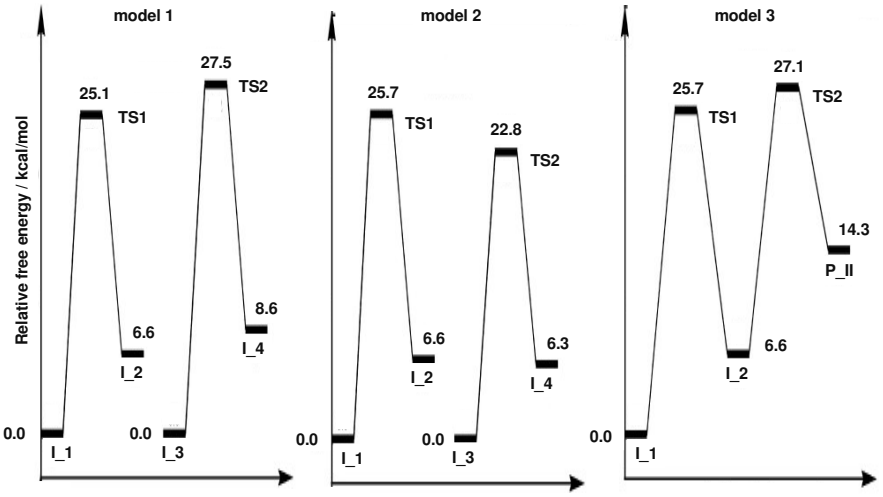

Figure 3.17: Free energy profiles for the hydrolysis process of JM118 using model systems one to three, from left to right.

3.7 Paper IV

This paper present a preliminary study on cisplatin's activation and its subsequent reactions with DNA bases adenine and guanine, i.e. the reactions studied were those of paper II and the attack of diaquated cisplatin on a simple model of DNA. In addition the paper contains a section on the photochemistry of psoralen compounds. That part will not be included in this summary.

The DNA model in this study consisted of purine bases adenine and guanine and, although it is a small model, it should provide insight into the chemistry of the substitutions, without the added complexity of the surrounding parts of DNA. In this set of computations we have employed the pure DFT functional BLYP, in combination with the LanL2DZ basis set to obtain stationary points and frequencies of the reactions.

The reactions involving the activated cisplatin and the purine bases are very similar to the hydrolytic substitutions presented in paper I, with the main difference being the introduction of a hydrogen bond acceptor/donor on the purine base (O6 in guanine, N6 or its adherent hydrogens in adenine). The adduct bond lengths (i.e. between the purine N7 and Pt) are

experimentally determined to ~2.0 Å from X-ray crystallography and ~2.05 Å from NMR studies, whereas we find a value of 2.07 Å.

For the first purine substitution (reactions 1 and 2 in the paper II summary above), two types of reactant complexes with a corresponding transition state and product complex were found, which were dubbed conformer 1 and conformer 2, which in paper II are called path 1 and path 2 respectively, see figure 3.11. For an illustration of the geometries obtained at the stationary points see figure 3.12 of the paper II summary above. The main difference is the alignment of the purine hydrogen bond acceptors (N7 and O6/N6) to the diaquated cisplatin which is either to the two water ligands (conformer 1) or to one cisplatin ammine ligand and a water (conformer 2). In no case though, does the purine N7 coordinate to an ammine group hydrogen of cisplatin. All reactant complexes exhibit a partial proton transfer from a water ligand to N7 of the purine base, that is the proton is halfway between proton donor and acceptor. This acidity can, at least in part, be attributed to the electron attracting properties of the charged Platinum ion displacing the electron density of the ligands toward itself. Geometrically, the main differences between the complexes, when following the reactions toward the product, lie in the rotation and tilt of the attacking nucleobase. All other distances and angles are highly similar. Similarly to the aquation reactions, the magnitude of the imaginary frequencies of the transition states are very low (~150 cm^{-1}), indicating flat potential surfaces with low penalties energy-wise for geometries diverging from the computed TS when passing the activation energy barrier.

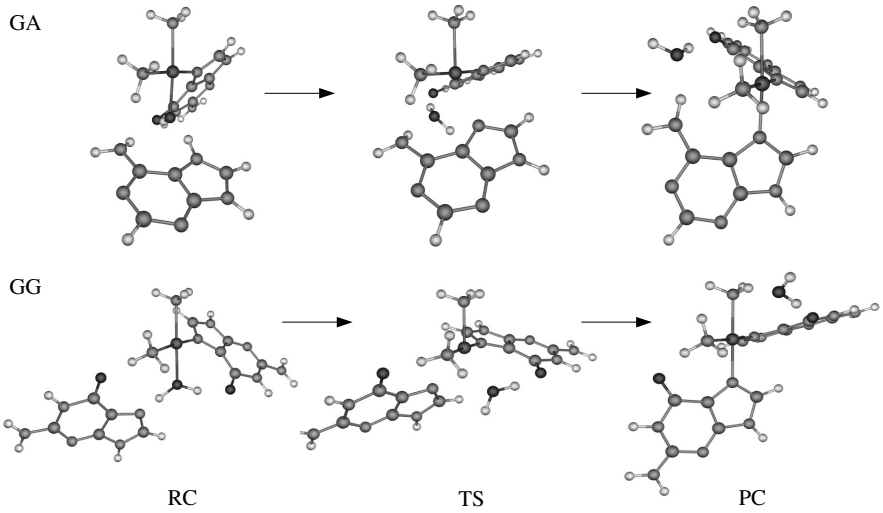

Figure 3.18: The second nucleobase substitution to cisplatin. Top row: Formation of GA product complex; bottom row: Formation of GG product complex.

The energy barriers for the first substitution are all very high, 35-40 kcal/mol, which is much too high for any significant amount of adduct to form under physiological conditions. The reason for this probably lies in the use of a small model in vacuum. There is however a systematic difference in energy between the two conformers amounting to ~7-10 kcal/mol. This is clearly related to the difference in interaction energy of the O6/N6-H2O hydrogen bond compared to the O6/N6-H3N hydrogen bond, and could constitute a selection criterion for the preferred route to a bifunctional adduct to DNA.

For the second substitution reaction (reaction 3 and 4 above), we have chosen to start from the guanine complex of conformer 1 only. The same basic geometrical features are observed as in the first substitution. However, an interesting difference between the two substitutions is the geometry of the two product complexes. Whereas the GA product complex (of reaction 4) reproduces the overall structure of an intrastand adduct (Head-to-Head) fairly well, the GG product complex (of reaction 3) more closely resembles that of an interstrand adduct (figure 3.18). The explanation to this is either found in the extended degrees of freedom this model provides, compared to the in vivo situation, or that the final structures strongly depend on the initial conformations.

Energetically these two reactions have very high barriers of activation, ~30 kcal/mol, with the GG system having a slightly lower barrier and is slightly more favoured thermodynamically than the AG system. The energetics alone do not explain the observed differences in product distribution. However, they do present a schematic view of the reactions taking place, the role of the different ligands, and the importance of stabilising hydrogen bonding and possible steric hindrance in the full DNA system.

4. Conclusions and outlook

In the pursuit of novel Platinum-based chemotherapeutic agents, it is becoming increasingly more evident that slavishly following the directives of long established SAR rules will not produce significant improvements on existing drugs. These rules have as a consequence been cast aside in recent research, attempting to overcome the weaker aspects of the original compound cisplatin and its second generation derivatives. When trying to rationally design next-generation Platinum drugs, it is paramount to have a deep and detailed understanding of the reactions these drugs undergo with relevant biomolecules. The work presented herein show that much of this understanding can be obtained using the tools of quantum chemistry.

In this work, an accurate model of the activation reactions cisplatin is subjected to has been developed that faithfully reproduce available experimental data. The model employed a combination of discrete, explicit solvation molecules and an implicit, continuum solvation model representing the bulk of the solvent. This model has subsequently been applied studying the activation reactions of a promising drug candidate, JM118, where the diaquated species was deemed more viable than in cisplatin's case. Diaquated Platinum species are more reactive toward the ultimate target, DNA, than corresponding monoaquated species. Capacity for diaquation of any candidate drug is therefore a desirable trait, since this maximizes the effect of the drug at all dosages. Using the model developed here, the inclination of novel drug candidates to form diaquated derivatives can be probed with relative ease and convenience.

The non-bonded interactions and chemical reactions between activated, diaquated cisplatin and its chief target nucleotides of DNA, guanine and adenine have also been studied here. The results obtained computationally are in very good accord with comparable experimental data. An alternative selection criterion to the previously suggested kinetic argument for the bias of cisplatin toward binding to guanine is proposed, based on the systematic difference in complexation energy of the cisplatin-adenine and cisplatin-guanine reactant complexes. The difference is found to strongly favour guanine binding, both in the monofunctional and the bifunctional adduct formation. In addition, an explanation to the observed directionality of the 1,2-d(ApG) bifunctional adduct is inferred based on this result. The viability of a drug candidate can be gauged using the methodology developed in this investigation, partly in terms of kinetic feasibility using data

from activation barrier height determinations but also through the thermodynamic stability of the products of these reactions, which can provide an estimate on the longevity of putative bonds to DNA.

Going forward, there are obvious limitations with an all quantum description of these interactions and reactions, mainly related to the size of the model systems that can feasibly be studied. Even the most beneficially scaling method scales formally to the fourth power with system size[†], which puts an effective size limit on the systems possible to study. In the present case – cisplatin interactions with DNA – this has meant that adjacent portions of DNA have not been included and the possible influence that may have had is therefore ignored. While not at all disqualifying the results this is somewhat unsatisfying. This issue can at present best be addressed by hybrid quantal-classical methods.

Having a working, reliable quantum mechanical/molecular mechanical (QM/MM) model would enable other than nominal extensions of the system size permitting the calculation of what influence adjacent parts of DNA would have on the chelation process, both for existing drugs and drugs *in spe*, since there are outstanding questions which have not so far been thoroughly addressed. For instance, why are certain sequences of DNA more susceptible to initial attack, and consequentially adduct closure?

Also in the absence of a working QM/MM model much fundamental research can still be performed using traditional quantum chemical methods. In the interest of rationally designing new Platinum-base cancer drugs, there is a lack of data on the effect of systematically altered carrier ligands. This can be addressed by traditional means. For instance, the effect of various amines instead of ammines as carrier ligands on the activation barriers of aquation can be obtained in this way. These effects are of interest for one of the lines of investigation currently pursued, trying to design complexes where access to the Platinum ion is sterically hindered by bulky groups on the carrier ligands. One purpose of these bulky groups is to evade cellular detoxification molecules metallotionein and glutathione implicated in cisplatin resistance.

But for some formidable breakthrough in hardware or software, the role of quantum chemistry in developing novel drugs has never been, and will likely not become in the foreseeable future, that of a drug discovery tool in its own right. Rather it has the role of providing fundamental and detailed knowledge of chemical properties and reactions when and where such is hard to obtain by other means. In that it excels however, and with a bit of luck the above assertion about the fitness of quantum chemistry as a drug discovery tool will be disproved [‡].

[†]The number of electrons.

[‡]Come that day I will ask for a serious raise.

Summary in Swedish

Kvantkemiska Studier av det Cytostatiska Läkemedlet Cisplatin

Aktivering och Bindning till DNA

Cisplatin är en tämligen liten, oorganisk molekyl vars oansenliga yttre inte på något sätt röjer dess starka cytotoxiska egenskaper. Denna cytotoxicitet har gjort cisplatin till ett av de mest använda cancerläkemedlen till dags dato.

Cisplatins kemiska formel fastställdes 1845 av Michel Peyrone och dess moleylära struktur bestämdes 1893 av Alfred Werner, en gigant inom strukturkemi och sedemera nobelpristagare i kemi, i en mycket inflytelserik artikel. Det Werner upptäckt var att cisplatin, då känt under namnet Peyrones klorid*, hade en kvadratiskt plan struktur där Platina centralt i kvadraten koordinerade fyra ligander mot hörnen av kvadraten. Liganderna består av två ammoniakmolekyler och två negativt laddade kloridjoner i en så kallad *cis-* konfiguration, vilket generellt betecknar att två identiska grupper – ligander i cisplatins fall – befinner sig på samma sida om ett tänkt plan, se figur 3.1, där det tänkta planet är horisontellt och vinkelrätt mot pappret. Platina är i oxidationstillstånd 2+, formellt skrivet Pt(II), och molekylen är alltså neutral inräknat kloridjonerna.

Fram till cisplatins återupptäckt 1965, skedde egentligen bara en vetenskaplig upptäckt av vikt gällande cisplatin. Förklaringen till den kvadratiskt plana strukturen som ges av kvantmekaniken och innebär att attraktionen mellan den positivt laddade platinajonen och de negativa liganderna†, eller den negativa delen av dem‡, är starkast då de är arrangerade i en kvadratiskt plan geometri kring platinajonen. En likvärdig formulering av samma sak är att denna geometri ger lägst potentiell energi för molekylen, dvs. den är i maximal ”vila”.

Upptäckten av cisplatins cytotoxicitet 1965 var en mycket lyckosam slump. Ett experiment, fullständigt orelaterat cancer, utfördes på *Escherichia Coli* bakterier, där bakterierna odlades i ett oscillerande elektriskt fält. I enlighet med kemiskt sunt förnuft elektroder av Platina valts att sänkas ned i bakterielösningen, eftersom Platina är kemiskt inert – eller så trodde man åtminstone. Ganska snart efter experimentets början

* Ibland kan man även se beteckningen “Peyrones salt”.

† I cisplatins fall kloridjonerna

‡ De polära ammoniakliganderna i cisplatin

upptäcktes att bakteriernas tillväxt ändrade karaktär och de blev avlånga, vilket är ett säkert tecken på att celldelningen hos *E. Coli* hindrats.

Efter en serie undersökningar där möjliga orsaker till fenomenet uteslöts en efter en, befanns slutligen den avbrutna celldelningen vara följden av substanser tillkomna genom en elektrolytisk reaktion med elektroderna, däribland cisplatin, som visade sig vara den mest aktiva av substanserna. En validerings process följde och småningom godkändes cisplatin av amerikanska FDA 1978 för behandling av testikel-, äggstock- och urinvägscancer.

Cisplatins kliniska effekt uppnås, liksom för många andra cytostatika, genom att den skenande celldelningsprocessen hos tumörcellerna hämmas eller stoppas genom att DNA modifieras i ett eller annat avseende. Eftersom den metaboliska takten i tumörceller är kraftigt förhöjd slår DNA-modifierande substanser mycket hårdare mot tumörceller än kroppens övriga celler[†].

Man kan tycka att under de över trettio år som gått sedan upptäckten borde många förbättringar ha gjorts på cisplatin men så är inte fallet. Frågan man ställer sig därför är naturligtvis varför, eller mer specifikt; vad är det som får cisplatin att fungera så bra att vi inte sett några genomgripande förbättringar på dessa trettio år? Fundamental och detaljerad kunskap om cisplatins verkan är därför en nödvändighet.

När man eftersöker detaljerad och precis data om fysisk växelverkan och kemiska reaktioner är kvantkemin ofta det naturliga valet av verktyg. Denna avhandling är en kvantkemisk studie av cisplatins bindning till DNA och de reaktioner som föregår detta. Kvantkemi är den gren inom kemin där fysik och matematik tillämpas på kemiska problem. Den främsta styrkan hos kvantkemin är att mycket detaljerad information kan fås om de frågeställningar man studerar. Denna styrka blir särskilt uttalad i fall där det är svårt eller till och med omöjligt att anskaffa informationen på annat sätt. Ett exempel är flyktiga kemiska tillstånd som i de flesta fall är omöjliga att få detaljerad information om experimentellt.

Vid 1900-talets början stod det klart för fysikerna att någonting var fel. Atomens beståndsdelar hade nyligen upptäckts och man fann snart att den etablerade fysiken inte kunde beskriva beteendet hos dessa partiklar. Speciellt tydligt var detta för elektronen som under vissa förhållanden existerade som en våg, under andra som en fast partikel. Denna våg-partikeldualism medförde att den klassiska, Newtonska fysiken inte räckte för att beskriva elektronerna utan ny teori måste till, kvantmekaniken.

Den viktigaste konsekvensen av elektronens vågegenskaper är att den omgivning elektronen befinner sig i definierar utseendet på vågen. Man kan

[†]Undantag finns. Däribland hårsäcksceller och tarmepitelceller där celldelningstakten är mycket hög även normalt sett. Håravfall och diarréer är därför mycket vanliga bieffekter av cytostatika.

jämföra det vid en gitarrsträng där tonen (utseendet på vågen) bestäms av längden på strängen och hur spänd den är. Motsvarigheten till stränglängd och spänning för elektronvågen är den elektrostatiska potential elektronen befinner sig i. Denna potential utgörs i reella fall av interaktionen med andra laddade partiklar och kan vara antingen attraktiv eller repulsiv, t.ex. attraktionen till den positivt laddade kärnan i en atom eller repulsionen från en annan elektron.

Potentialen avgör alltså hur elektronens vågfunktion ska se ut, vilket ger upphov till en familj av tillåtna vågfunktioner, som för atomer och molekyler kallas orbitaler. Strikt räknat kan man bara finna exakta orbitaler för väteatomen och man får i andra fall förlita sig på approximativa, men mycket noggranna, sätt att hitta vågfunktionerna där användandet av datorer är en absolut nödvändighet. När man beräknat orbitalerna har man också möjligheten att räkna ut på vilket sätt de interagerar med varandra då man förändrar potentialen, d.v.s. man kan räkna ut hur en kemisk reaktion går till genom att ändra atomkärnornas läge. Moderna metoder för att finna elektroniska vågfunktioner i molekyler och atomer har i kombination med den osannolikt snabba utvecklingen av datorer och deras tillgänglighet gjort det möjligt att nu behandla molekyler och reaktioner av en storlek som för bara några år sedan tedde sig som fantasier. Det är denna utveckling som möjliggjort denna studie.

Denna avhandling undersöker de kemiska reaktioner cisplatin genomgår, dels med cisplatins kliniska mål DNA – det som gör det verksamt mot cancer – och dels de reaktioner som föregår detta. I tillägg redovisas också en undersökning av de aktiveringsreaktioner ett cisplatinbaserat kandidatläkemedel genomgår innan bindningen till DNA.

Cisplatin binder till DNA genom att två av dess ligander successivt byts ut mot två DNA baser, guanin alternativt adenin, med en stor övervikt för bindning till guanin. Den vanligaste bindningen är till två intilliggande guaninbaser i DNA och därefter vanligast är till en adenin-guanin följd där riktningen alltid är 5'-AG-3'. Riktningsspecificiteten har en av de häri redovisade undersökningarna föreslagit en förklaring till. De ovan nämda skadorna på DNA korrelerar till den cytostatiska verkan hos cisplatin.

Cisplatin kan sägas vara proto-läkemedlet för alla efterföljande Platinabaserade cancerläkemedel av orsaken att den DNA-bindande enheten hos dessa, kandidatläkemedel likväl som godkända, undantagslöst är en kvadratisk-plan Platina-enhet i likhet med cisplatin. Detta gör att resultaten och modellerna från de häri redovisade undersökningarna har stor, om än i vissa fall indirekt, relevans för alla Platinabaserade läkemedel.

När cisplatin passerat cellmembranet och kommit in i cytoplasman möter den en klart minskad koncentration av kloridjoner, jämfört med blodbanans, vilket gör cisplatins kloridligander mottagliga för substitution med vattenmolekyler. En eller två kloridligander byts därvid ut i cisplatin och detta *aktiverar* läkemedlet, dvs. den kliniskt verksamma reaktionen

med DNA möjliggörs. Kvantkemiska beräkningar har genomförts på dessa substitutioner där två modeller använts: Ett minimalt system där endast de reagerande molekylerna inkluderats och ett där ett partiellt lager av molekyler från lösningsmedlet (vatten) inkluderats tilläggsvis. Beräkningarna visade god överrensstämmelse med experimentella data. Resultatet av undersökningen visade också att den gängse uppfattningen att cisplatin genomgår en substitution med vatten innan det binder till DNA har gott fog för sig. Det visade sig också att det minimala systemet var mindre lämpat än det större som modellsystem betraktat.

Metodiken som utarbetats i studien ovan användes däefter i undersökningen av ett lovande, platinabaserat kandidatläkemedel, JM118, som förhoppningsvis ska kunna tas via munnen till skillnad från cisplatin. En väsentlig skillnad befanns i denna studie vara att JM118 skulle ha betydligt lättare att bilda ett dubbelt vattensubstituerat komplex än cisplatin. Detta utgör en fördel gentemot cisplatin eftersom dubbelt substituerade platinakomplex är mer reaktiva mot DNA.

Slutligen har de reaktioner som sker mellan DNA och dubbelt substituerat cisplatin studerats. Modellsystemen bestod av DNA baserna adenin och guanin samt dubbelsubstituerat cisplatin. Den initiala reaktionen mellan cisplatin och basen visade sig vara mest fördelaktig mellan guanin och cisplatin i avseendet att mindre energi krävdes i detta fall, i enlighet med experimentella observationer. Dessutom befanns det finnas en systematisk skillnad i interaktionsenergin som föregick reaktionssteget. En skillnad som även den påvisade en predisposition för cisplatin att binda till guanin. Från detta resultat kan även riktningsspecifiteten 5’-3’ hos kelatprodukten 5’-AG-3’ härledas.

Sammanfattningsvis kan sägas att de presenterade studierna har lämnat bidrag till vår kunskap om de aktiveringsreaktioner cisplatin genomgår innan bindningen till DNA, och för dessa utvecklat en modell som kan tillämpas på nya cisplatinbaserade kandidatläkemedel, vilket har visats i undersökningen av det lovande kandidatläkemedlet JM118. Vidare har beräkningar på de reaktioner aktiverat cisplatin genomgår med DNA nukleotiderna guanine och adenine påvisat en alternativ förklaring till den observerade preferensen för bindning till guanine, utgående från den beräknade skillnaden i stabilitet som de initiala komplexen uppvisar. Detta ger också en förklaring till riktningsspecificiteten i den näst vanligaste bindningen cisplatin bildar till DNA, 5’-AG-3’.

Acknowledgements

Many people have directly and indirectly enabled the making of this thesis. I would like to start with a special thank you regarding the work in direct connection to the writing of this thesis, quite aside from other reasons I have to feel grateful. I am much obliged for the help and support of my supervisor Dr. David van der Spoel and the constructive attitude he always displays in matters high and low. I am also thankful for his gently suggesting me to use LaTeX when writing this thesis. This may seem trivial but it really has been a life saver. A big thank you goes to Dr. Nicuşor Tîmneanu for his diligent scrutiny of the theoretical section of the thesis. Your eye for detail and structure alike have been a source of many gray hairs. I would like to thank to Prof. Janos Hajdu for his many kind words of encouragement and for helping me see the broad strokes*. If "motivational skills" were an olympic event you should definitely enter.

I gratefully acknowledge the skillful editing and the discussions on our articles, as well as the generous contributions to conferences, of my former supervisor Prof. Leif A. Eriksson for the benefits this have brought to the papers presented in this thesis.

My old "compadre" Bobbo deserves a big hug and a heartfelt thank you for good friendship, lots of good, clean fun on conferences and for sharing the same set of vices as me. Well, you're actually a lot worse my friend – or maybe not come to think of it – but that's neither here nor there.

I want to thank my roommate at BMC, Sara Lejon for her sense of humour. We share that sense so I know for a fact it's *great*.

A more general thanks goes to past and present members of the Molecular Biophysics group for the positive and easygoing atmosphere you have created throughout the years. I would like to mention a few specifically who I have enjoyed the company of for several years. In no particular order: The metal duo Magnus Bergh and Calle Caleman, Gösta Huldt, Alexandra Patriksson, Michiel van Lun, Filipe Maia, Karin Valegård, Marvin Seibert, Anke Terwisscha van Scheltinga and Martin Svenda. A special thank you in this category goes to Remco Wouts for invaluable assistance with many a computer issue and for his tenacity in our, completely work-unrelated, loudspeaker project which would never have got off the ground without his help.

*Yes, it's an idiom. :-)

Slutligen vill jag tacka min familj som har bistått på för många sätt att nämna under speciellt det sista året. Jag vill tacka mina föräldrar särskilt för omhändertagandet av Floyd (vår hund) periodvis under det gångna året, vilket har lyft en tung börda från mina axlar.

Mest av allt vill jag tacka Åsa för den förståelse och osjälviskhet hon visat så att jag kunnat skriva denna avhandling. Det hade *aldrig* gått annars. Jag vill också tacka min dotter Alice för hennes breda leende.

References

[1] Mosl, G. J. and Motzer, R. J. *N. Engl. J. Med.* **337**, 242–253 (1997).

[2] Cleare, M. J. and Hoeschele, J. D. *Plat. Met. Rev.* **17**, 3 (1973).

[3] Cleare, M. J. and Hoeschele, J. D. *Bioinorg. Chem.* **2**, 187 (1973).

[4] Heitler, W. and London, F. *Z. Physik* **44**, 455 (1927).

[5] Roothaan, C. C. J. *Rev. Mod. Phys.* **23**, 69 (1951).

[6] Hall, G. G. *Proc. R. Soc. (London)* **A205**, 541 (1951).

[7] Hartree, D. R. *Proc. Camb. Phil. Soc.* **24**, 89 (1928).

[8] Slater, J. C. *Phys. Rev.* **34**, 1293 (1929).

[9] Fock, V. *Z. Physik* **61**, 126 (1930).

[10] Thomas, L. H. *Proc. Camb. Phil. Soc.* **23**, 542 (1927).

[11] Fermi, E. *Rend. Accad. Lincei* **6**, 602 (1927).

[12] Fermi, E. *Z. Physik* **48**, 73 (1928).

[13] Dirac, P. A. M. *Proc. Camb. Phil. Soc.* **26**, 376 (1930).

[14] Szabo, A. and Ostlund, N. S. *Modern Quantum Chemistry.* McGraw-Hill, Inc., 1st revised edition, (1989).

[15] Parr, R. G. and Yang, W. *Density-Functional Theory of Atoms and Molecules.* Oxford University Press, Inc., 1st edition, (1989).

[16] Jensen, F. *Introduction to Computational Chemistry.* John Wiley & Sons Ltd., Chichester, 1st edition, (1999).

[17] Koch, W. and Holthausen, M. C. *A Chemist's Guide to Density Functional Theory.* Wiley-VCH Verlag GmbH, Weinheim, 2nd edition, (2002).

[18] Born, M. and Oppenheimer, R. *Ann. Physik* **84**, 457 (1927).

[19] Löwdin, P.-O. *Adv. Chem. Phys.* **2**, 207 (1959).

[20] Hohenberg, P. and Kohn, B. *Phys. Rev. B* **136**, 864 (1964).

[21] Kohn, W. and Sham, L. J. *Phys. Rev. A* **140**, 1122 (1965).

[22] Vosko, S. H., Wilk, L., and Nusair, M. *Can. J. Phys.* **58**, 1200 (1980).

[23] Becke, A. D. *Phys. Rev. B* **38**, 3098 (1988).

[24] Becke, A. D. *J. Chem. Phys.* **98**, 5648 (1993).

[25] Cramer, C. J. *Essentials of Computational Chemistry*, chapter 8, 260 – 269. John Wiley & Sons Ltd., Chichester, 1st edition (2002).

[26] Lee, C., Yang, W., and Parr, R. G. *Phys. Rev. B* **37**, 785 (1988).

[27] Stevens, P. J., Devlin, F. J., Chabalowski, C. F., and Frisch, M. J. *J. Phys. Chem.* **98**, 11623 (1994).

[28] Leffler, J. E. *Science* **117**, 340–341 (1952).

[29] Hammond, G. S. *J. Am. Chem. Soc.* **77**, 334–338 (1955).

[30] Miertus, S., Scrocco, E., and Tomasi, J. *Chem. Phys.* **55**, 117 (1981).

[31] Miertus, S. and Tomasi, J. *Chem. Phys.* **65**, 239 (1982).

[32] Rosenberg, G., Camp, L. V., and Krigas, T. *Nature* **205**, 698 (1965,).

[33] Rosenberg, B., Camp, L. V., Trosko, J. E., and Mansour, V. H. *Nature* **222**, 385 (1969).

[34] Lebwohl, D. and Canetta, R. *Eur. J. Cancer* **34**, 1522 (1998).

[35] Giandomenico, C. M., Abrams, M. J., Murrer, B. A., Vollano, J. F., Harrap, K., Goddard, P. M., Kelland, L. R., and Morgan, S. E. *Platinum and Other Metal Coordination Compounds in Cancer Chemotherapy*, 93–100. Plenum Press: New York (1991).

[36] Sternberg, C. N., Hetherington, J., Paluchowska, P. H. T., Slee, J., Collette, L., Debois, M., and Zurlo, A. *Proc. Am. Soc. Clin. Oncol.* **22**, 395 (2003).

[37] Farrell, N. P., Almeida, S. G. D., and Skov, K. A. *J. Am. Chem. Soc.* **110**, 5018–5019 (1988).

[38] Qu, Y., Appleton, T. G., Hoeschele, J. D., and Farrell, N. P. *Inorg. Chem.* **32**, 2591–2593 (1993).

[39] Sharp, S. Y. and Kelland, L. R. *Curr. Opin. Oncol. Endocr. Metabol. Invest. Drugs* **2**, 353–360 (2000).

[40] Peyrone, M. *Ann.* **51**, 15 (1845).

[41] Werner, A. *Z. Anorg. Chem.* **3**, 267 (1893).

[42] Bethe, H. *Ann. Physik* **3**, 133–206 (1929).

[43] Vleck, J. H. V. *The Theory of Electric and Magnetic Susceptibilities*. Oxford University Press, (1932).

[44] Rosenberg, B. *Nucleic Acid-Metal Ion Interactions.*, volume 1, chapter 1, 1–29. John Wiley & Sons, Inc.: New York (1980).

[45] Adler, H. I. and Hardigree, A. A. *Rad. Res.* **25**, 92–102 (1965).

[46] Witkin, E. M. *Proc. Natl. Acad. Sci.* **57**, 1275–1279 (1967).

[47] Andrews, P. A., Mann, S. C., Velury, S., and Howell, S. B. *Platinum and other metal coordination compounds in cancer chemotherapy*, 248–254. Martinus Nijhoff Publishing; Boston (1988).

[48] Davies, M. S., Berners-Price, S. J., and Hambley, T. W. *Inorg. Chem.* **39**, 5603 (2000).

[49] Legendre, F., Bas, V., Kozelka, J., and Chottard, J.-C. *Chem. Eur. J.* **6**, 2002 (2000).

[50] Douglas, B., McDaniel, D. H., and Alexander, J. J. *Concepts and Models of Inorganic Chemistry*. John Wiley & Sons Ltd., Chichester, 1st edition (1983).

[51] Hall, A. J. and Satchell, D. P. N. *J. Chem. Soc., Dalton Trans.* **6**, 1403 (1977).

[52] Bolster, M. W. G. D., Cammack, R., Coucouvanis, D. N., Reedijk, J., and Veeger, C. J. *Biol. Inorg. Chem.* **1**, G1 (1996).

[53] Perumareddi, J. R. and Adamson, A. W. *J. Phys. Chem.* **72**, 414 (1978).

[54] Stetsenko, A. I. and Scl'derkhanova, L. B. *Zh. Neorg. Khim.* **25**, 164 (1981).

[55] Bose, R. N., Cornelius, R. D., and Viola, R. E. *J. Am. Chem. Soc.* **106**, 3336 (1984).

[56] Hindmarsh, K., House, D. A., and Turnbull, M. M. *Inorg. Chim. Acta* **257**, 11 – 18 (1997).

[57] Miller, S. E. and House, D. A. *Inorg. Chim. Acta* **166**, 189 – 197 (1989).

[58] Milburn, G. H. W. and Truter, M. R. *J. Chem. Soc. A* **166**, 1609 (1966).

[59] Loehrer, P. J. and Einhorn, L. H. *Ann. Intern. Med.* **100**, 704 (1984).

[60] Giaccone, G. *Drugs* **59 suppl. 4**, 9 (2000).

[61] Wong, E. and Giandomenico, C. M. *Chem. Rev.* **99**, 2451–2466 (1999).

[62] Judson, I. and Kelland, L. R. *Drugs* **59 suppl.**, 29–36 (2000).

[63] Beck, D. J. and Brubaker, R. R. *J. Bacteriol.* **116**, 1247 (1973).

[64] Brouwer, J., van de Putte, P., Fichtinger-Schepman, A. M. J., and Reedijk, J. *Proc. Natl. Acad. Sci.* **78**, 7010 (1981).

[65] Beck, D. J., Popoff, S., Sancar, A., and Rupp, W. D. *Nucleic Acids Res.* **13**, 7395 (1985).

[66] Eastman, A. *Biochemistry* **25**, 3912 (1986).

[67] Fichtinger-Schepman, A. M. J., van Oosterom, A. T., Lohman, P. H. M., and Berends, F. *Cancer Res.* **47**, 3000 (1987).

[68] Lepre, C. A., Strothkamp, K. G., and Lippard, S. J. *Biochemistry* **26**, 5651 (1987).

[69] Gelasco, A. and Lippard, S. J. *Biochemistry* **37**, 9230 (1998).

[70] Takahara, P. M., Rosenzweig, A. C., Frederick, C. A., and Lippard, S. J. *Nature* **377**, 649 (1995).

[71] Coste, F., Malinge, J.-M., Serre, L., Shepard, W., Roth, M., Leng, M., and Zelwer, C. *Nucleic Acids Res.* **27**, 1837 (1999).

[72] Toney, J. H., Donahue, B. A., Kellett, P. J., Bruhn, S. L., Essigmann, J. M., and Lippard, S. J. *Proc. Natl. Acad. Sci.* **86**, 8328–8332 (1989).

[73] Donahue, B. A., Augot, M., Bellon, S. F., Trieber, D. K., Toney, J. H., Lippard, S. J., and Essigmann, J. M. *Biochemistry* **29**, 5872–5880 (1990).

[74] Bruhn, S. L., Pil, P. M., Essigmann, J. M., Housman, D. E., and Lippard, S. J. *Proc. Natl. Acad. Sci.* **89**, 2307–2311 (1992).

[75] Hughes, E. N., Engelsberg, B. N., and Billings, P. C. *J. Biol. Chem.* **276**, 13520–13527 (1992).

[76] Grosschedl, R., Giese, K., and Pagel, J. *Trends Genet.* **10**, 94 (1994).

[77] McA'Nulty, N. M. M. and Lippard, S. J. *Inorg. Chem.* **9**, 687 (1995).

[78] Ohndorf, U.-M., Rould, M., He, Q., Pabo, C., and Lippard, S. *Nature* **399**, 708 (1999).

[79] Reedijk, J. *Inorg. Chim. Acta* **198-200**, 873–881 (1992).

[80] Sherman, S. E., Gibson, D., Wang, A. H.-J., and Lippard, S. J. *Science* **230**, 412–417 (1985).

[81] Sherman, S. E., Gibson, D., Wang, A. H.-J., and Lippard, S. J. *J. Am. Chem. Soc.* **110**, 7368–7381 (1988).

[82] Mennucci, B. and Tomasi, J. *J. Chem. Phys.* **106**, 5151 (1997).

[83] Mennucci, B., Cancès, E., and Tomasi, J. *J. Phys. Chem. B* **101**, 10506 (1997).

[84] Tomasi, J., Mennucci, B., and Cancès, E. J. *Mol. Struct. (THEOCHEM)* **464**, 211 (1999).

[85] Carloni, P., Sprik, M., and Andreoni, W. *J. Phys. Chem. B* **104**, 823 (2000).

[86] Zhang, Y., Guo, Z., and You, X.-Z. *J. Am. Chem. Soc.* **123**, 9378 (2001).

[87] Car, R. and Parrinello, M. *Phys. Rev. Lett.* **55**, 2471 (1985).

[88] Remler, D. K. and Madden, P. A. *Mol. Phys.* **70**, 921 (1990).

[89] Kirkwood, J. G. *J. Chem. Phys.* **2**, 351 (1934).

[90] Onsager, L. *J. Am. Chem. Soc.* **58**, 1486 (1936).

[91] Hay, P. J. and Wadt, W. R. *J. Chem. Phys.* **82**, 270 (1985).

[92] Wadt, W. R. and Hay, P. J. *J. Chem. Phys.* **82**, 284 (1985).

[93] Hay, P. J. and Wadt, W. R. *J. Chem. Phys.* **82**, 299 (1985).

[94] MacLean, D. and Chandler, G. S. *J. Chem. Phys.* **72**, 5639 (1980).

[95] Krishnan, R., Binkley, J. S., Seeger, R., and Pople, J. A. *J. Chem. Phys.* **72**, 650 (1980).

[96] Arpalahti, J. and Lippert, B. *Inorg. Chem.* **29**, 104 (1990).

[97] Baik, M.-H., Friesner, R. A., and Lippard, S. J. *J. Am. Chem. Soc.* **125**, 14082 (2003).

[98] Bancroft, D. P., Lepre, C. A., and Lippard, S. J. *J. Am. Chem. Soc.* **112**, 6860 (1990).

[99] Blatter, E. E., Vollano, J. F., Krishnan, B. S., and Dabrowiak, J. C. *Biochemistry* **23**, 4817 (1984).

[100] van der Veer, J. L., Peters, A. R., and Reedijk, J. *J. Inorg. Biochem.* **26**, 137–142 (1986).

[101] Eastman, A. *Biochem. Pharmacol.* **36**, 4177 (1987).

[102] Pendyala, L., Cowens, J. W., Chheda, G. B., Dutta, S. P., and Creaven, P. J. *Cancer Res.* **48**, 3533 (1988).

[103] Pendyala, L., Krishnan, B. S., Walsh, J. R., Arakali, A. V., Cowens, J. W., and Creaven, P. J. *Cancer Chemother. Pharmacol.* **25**, 210 (1989).

[104] Gibbons, G. R., Wyrick, S., and Chaney, S. G. *Cancer Res.* **49**, 1402 (1989).

[105] Pendyala, L., Arakali, A. V., Sansone, P., Cowens, J. W., and Creaven, P. J. *Cancer Chemother. Pharmacol.* **27**, 248 (1990).

[106] Chaney, S. G., Gibbons, G. R., Wyrick, S., and Podhasky, P. *Cancer Res.* **51**, 969 (1991).

[107] Shi, T., Berglund, J., and Elding, L. I. *Inorg. Chem.* **35**, 3498 (1996).

[108] Bose, R. N. and Weaver, E. L. *J. Chem. Soc., Dalton Trans.* , 1797 (1997).

Acta Universitatis Upsaliensis

Digital Comprehensive Summaries of Uppsala Dissertations from the Faculty of Science and Technology 295

Editor: The Dean of the Faculty of Science and Technology

A doctoral dissertation from the Faculty of Science and Technology, Uppsala University, is usually a summary of a number of papers. A few copies of the complete dissertation are kept at major Swedish research libraries, while the summary alone is distributed internationally through the series Digital Comprehensive Summaries of Uppsala Dissertations from the Faculty of Science and Technology. (Prior to January, 2005, the series was published under the title "Comprehensive Summaries of Uppsala Dissertations from the Faculty of Science and Technology".)

Distribution: publications.uu.se
urn:nbn:se:uu:diva-7824

ACTA
UNIVERSITATIS
UPSALIENSIS
UPPSALA
2007